Surfin Board

Phys 476 Final Presentation

Ben Rotter
University of Hawaii at Manoa

ANITA ANTARCTIC IMPULSIVE TRANSIENT ANTENNA

UNIVERSITY OF HAWAI'I
MĀLAMALAMA
1907
UA MAU KE EA O KA 'ĀINA I KA PONO

ANITA-3

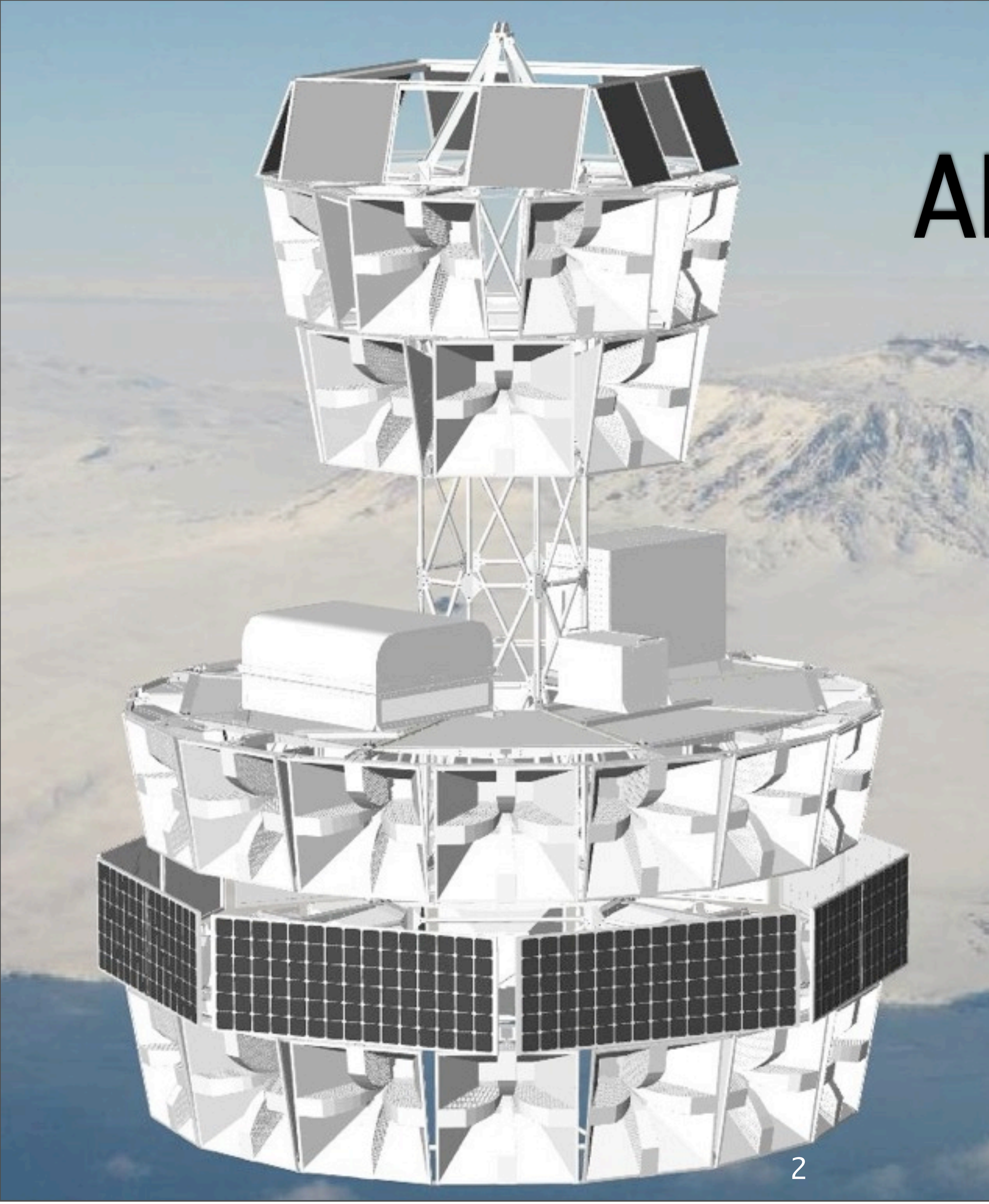

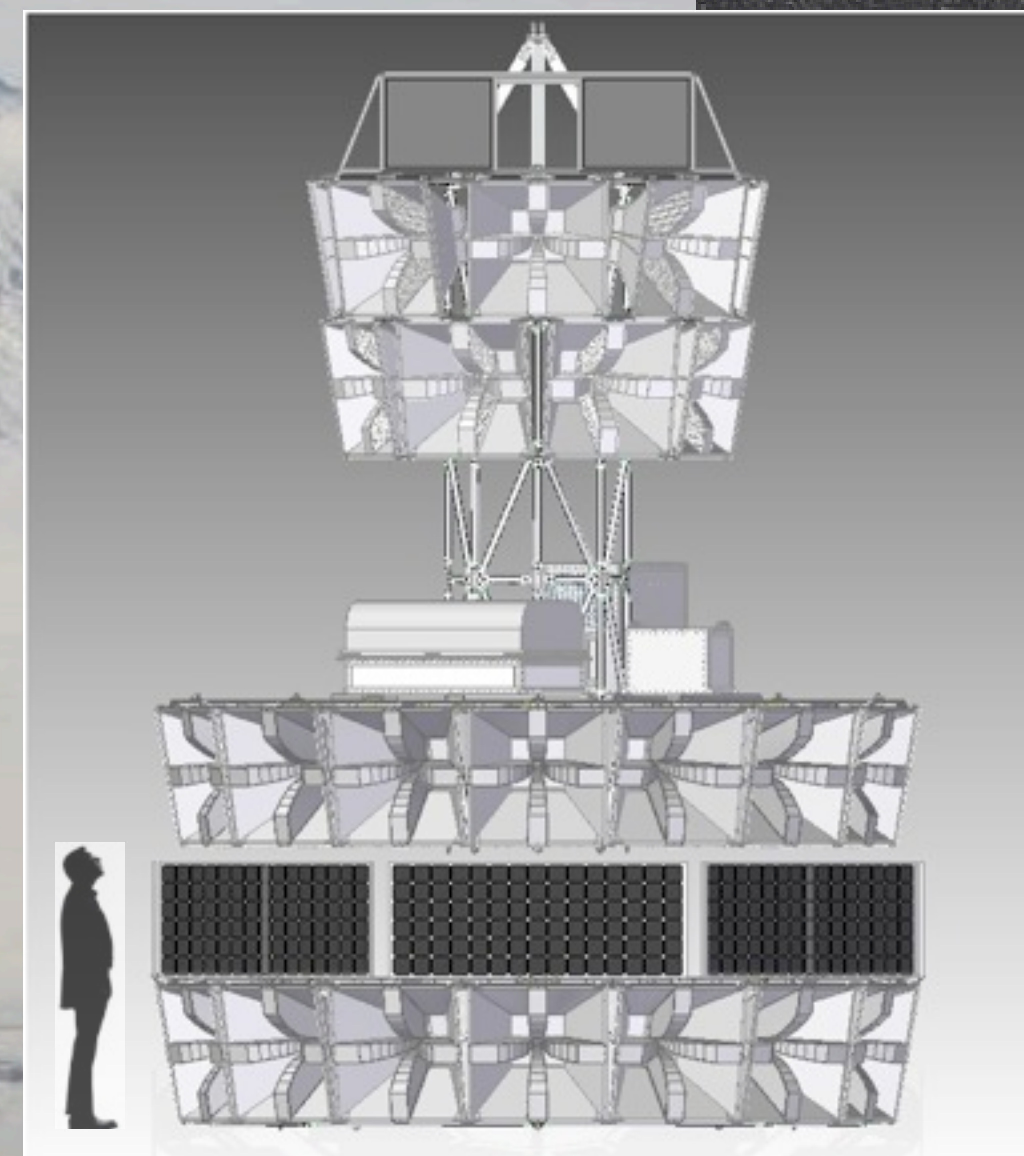

Detection Method

Particle interaction within ice emits radio transient captured by ANITA payload

Power detector senses dark matter interactions through increase in thermal noise level

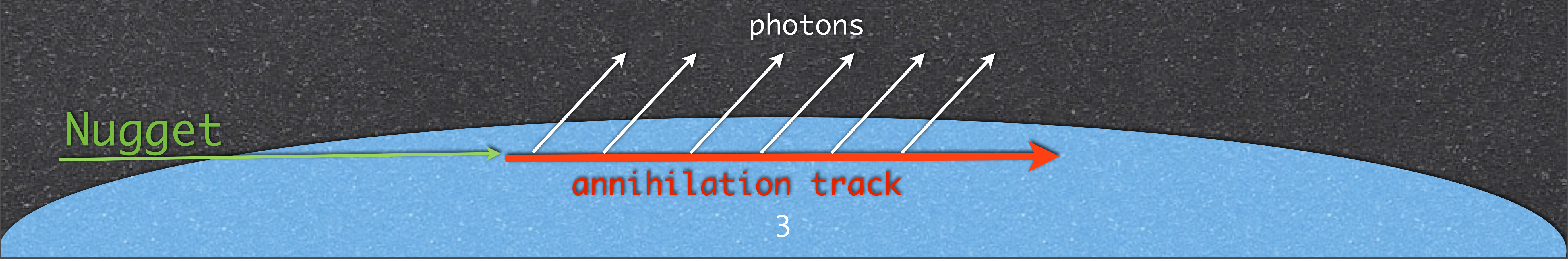

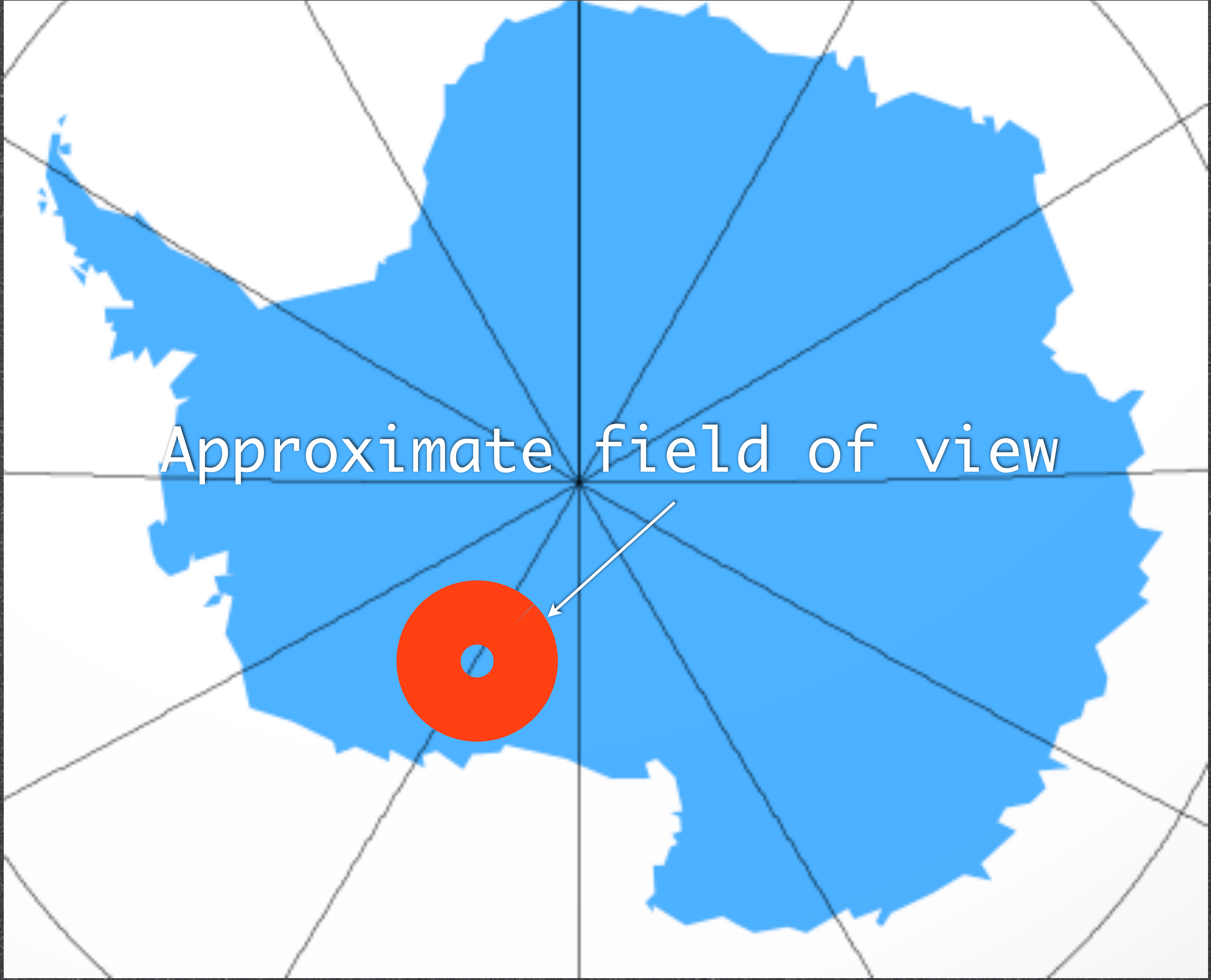
Approximate field of view

Theory: Anti-quark Nuggets

Antiquark nuggets as dark matter: New constraints and detection prospects

Peter W. Gorham[1]

[1] *Dept. of Physics & Astronomy, Univ. of Hawaii, Manoa, HI 96822.*

Current evidence for dark matter in the universe does not exclude heavy composite nuclear-density objects consisting of bound quarks or antiquarks over a significant range of masses. Here we analyze one such proposed scenario, which hypothesizes antiquark nuggets with a range of $B \sim 10^{24-30}$ with specific predictions for spectral emissivity via interactions with normal matter. We find that, if these objects make up the majority of the dark matter density in the solar neighborhood, their radiation efficiency in solids is marginally constrained, due to limits from the total geothermal energy budget of the Earth. At allowed radiation efficiencies, the number density of such objects can be constrained to be well below dark matter densities by existing radio data over a mass range currently not restricted by other methods.

- “Standard-model” candidate for Dark Matter
- Hypothesized as “strangelets” by Edward Witten in 1984
  - Modifications have been proposed more recently

Current Limits

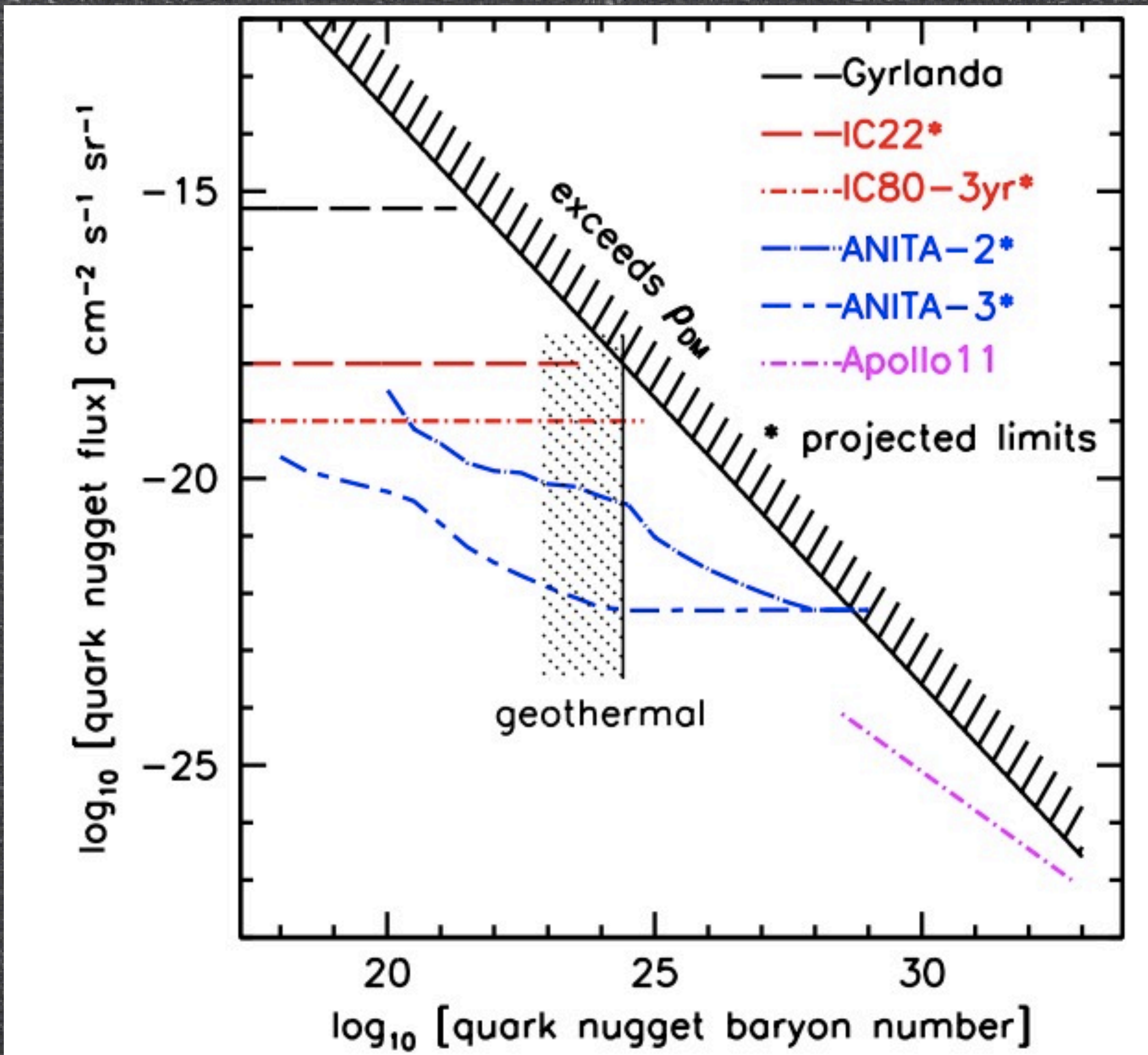

- Energy budget for geothermal activity in Earth and Moon
- Dark matter density
- Observations by IceCube and Lake Baikal Detector
- Observations by previous ANITA flights

Gorham arxiv:1208.3697

Why?

- Minor alterations to existing ANITA flight electronics needed for significantly improved sensitivity

Great return on investment!

ANITA 3 side view

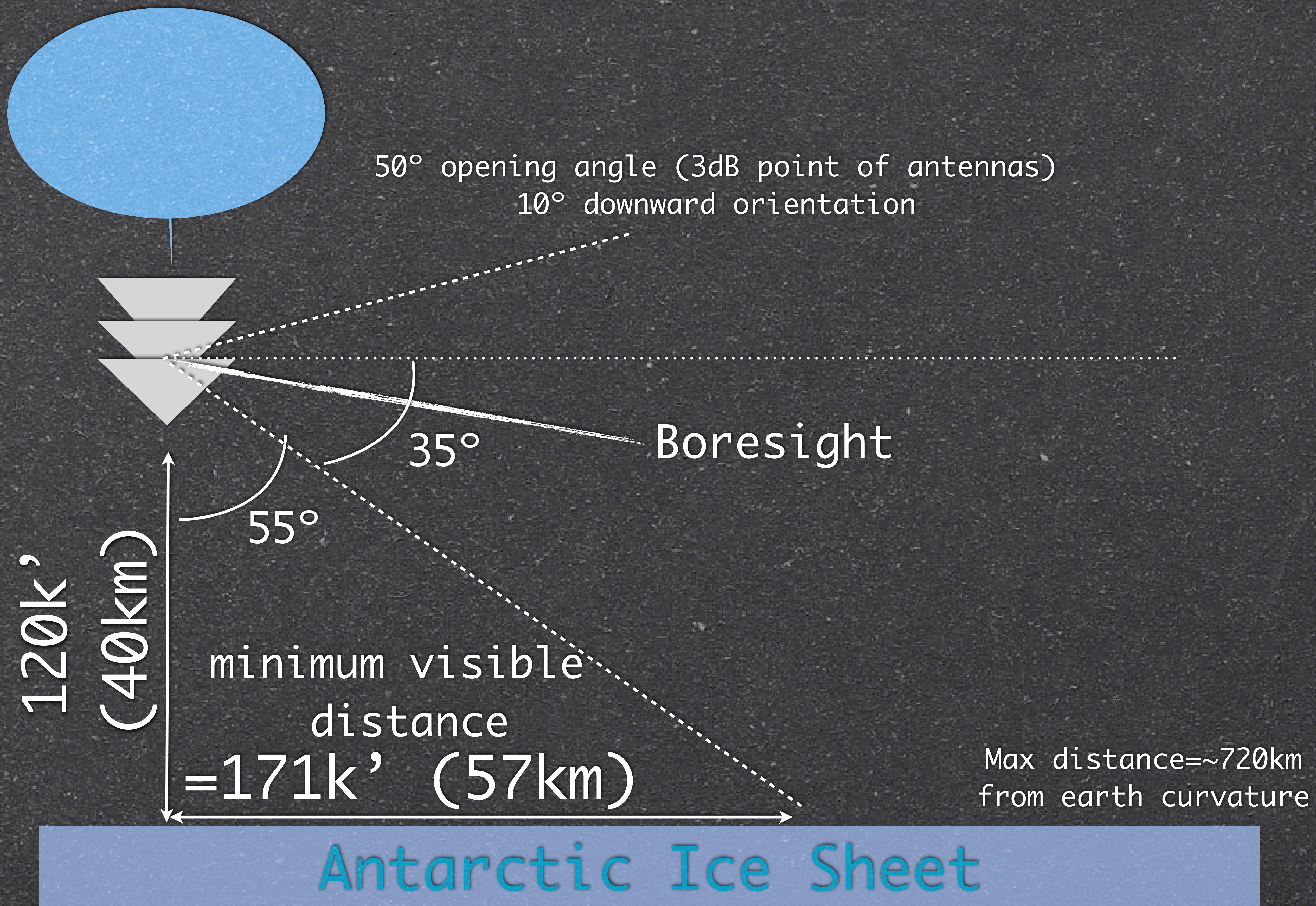

Phi Sectors

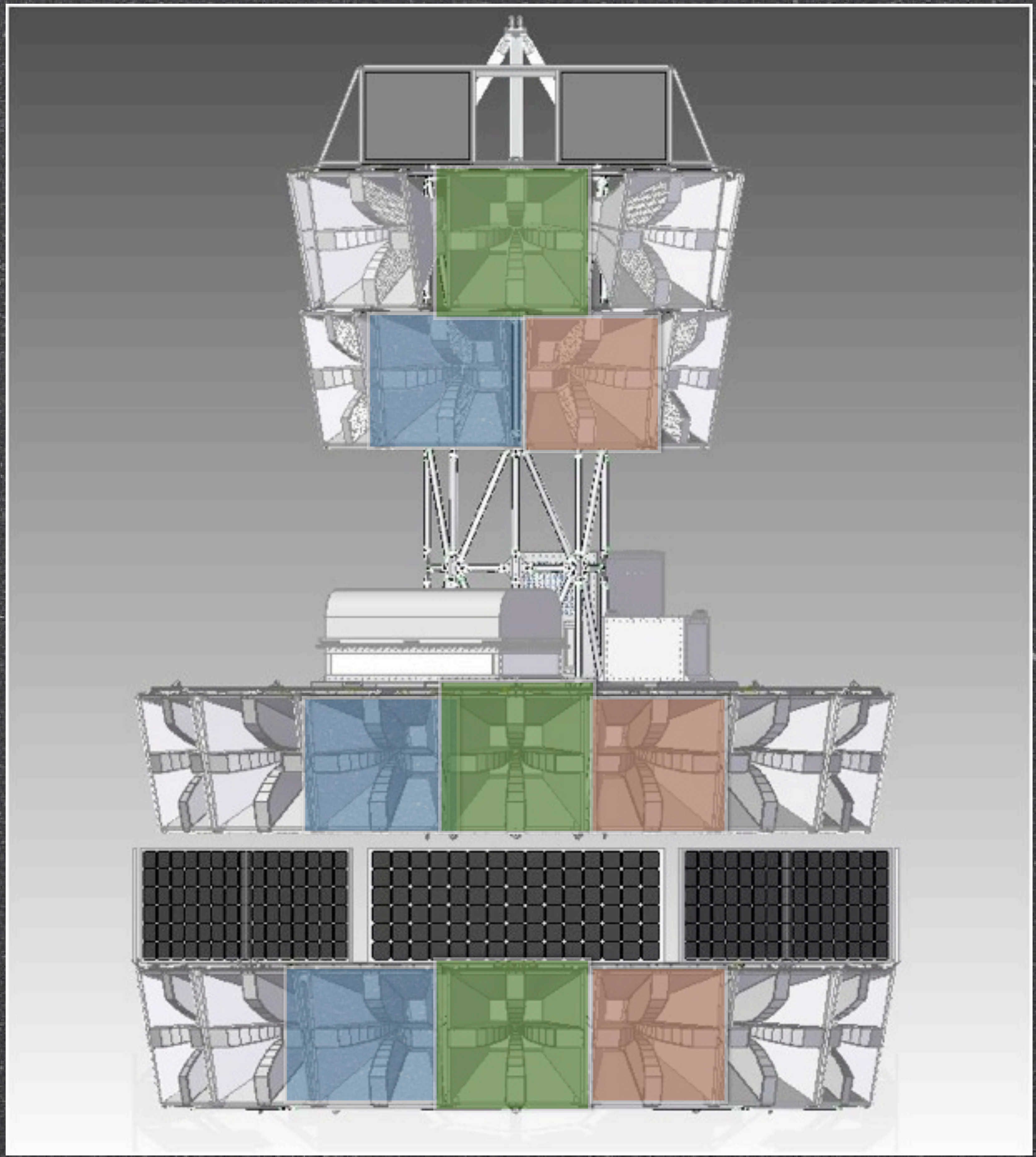

Top view

22.5° between
adjacent phi sectors

50° opening angle (minimum)

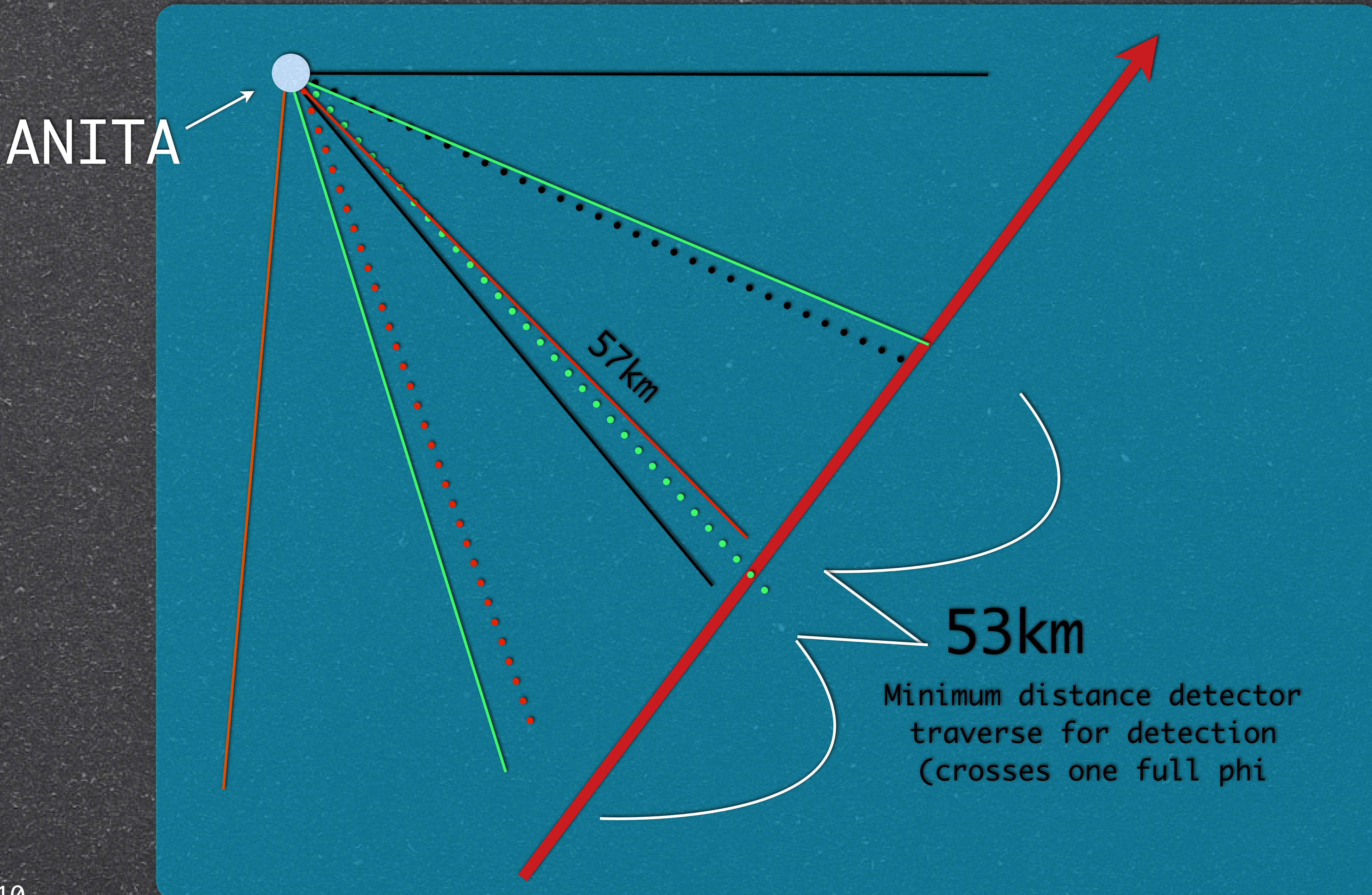

Two power monitors per antenna plus three antennas per phi sector provide spacial granularity

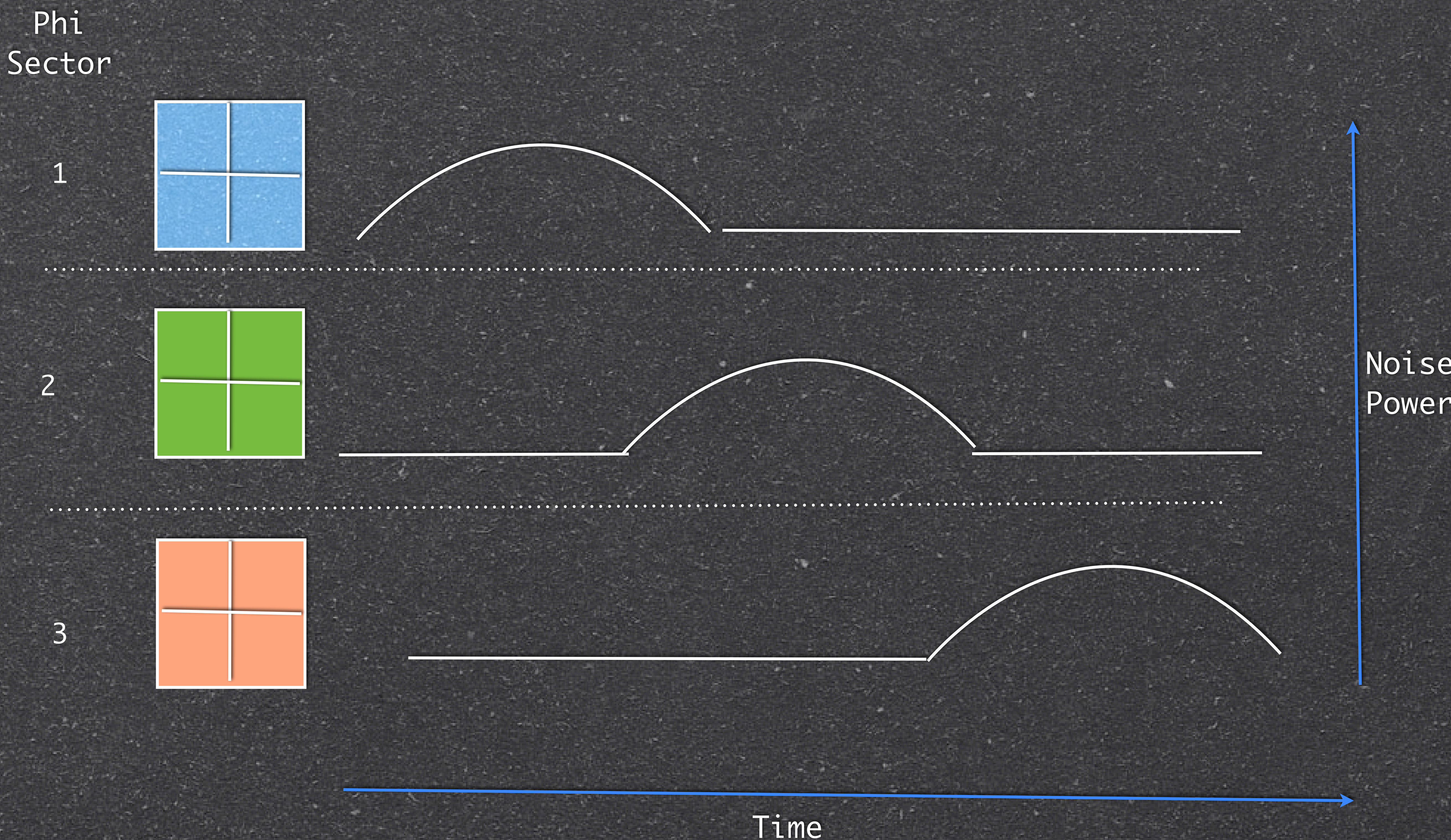

Improvements to ANITA2

- Unfortunate sampling scheme on ANITA-2 limited sensitivity of detector to dark matter
  - RF Power only measured upon readout of waveform detector, used as “aliveness” and gain monitor
  - 10Hz sampling rate, 1us integration time xxxxxxxx
- Increase sampling rate and integration time

Sampling rate vs event velocity

Sampling rate required to get 5 samples of an event moving at velocity V across detector to cross three phi sectors

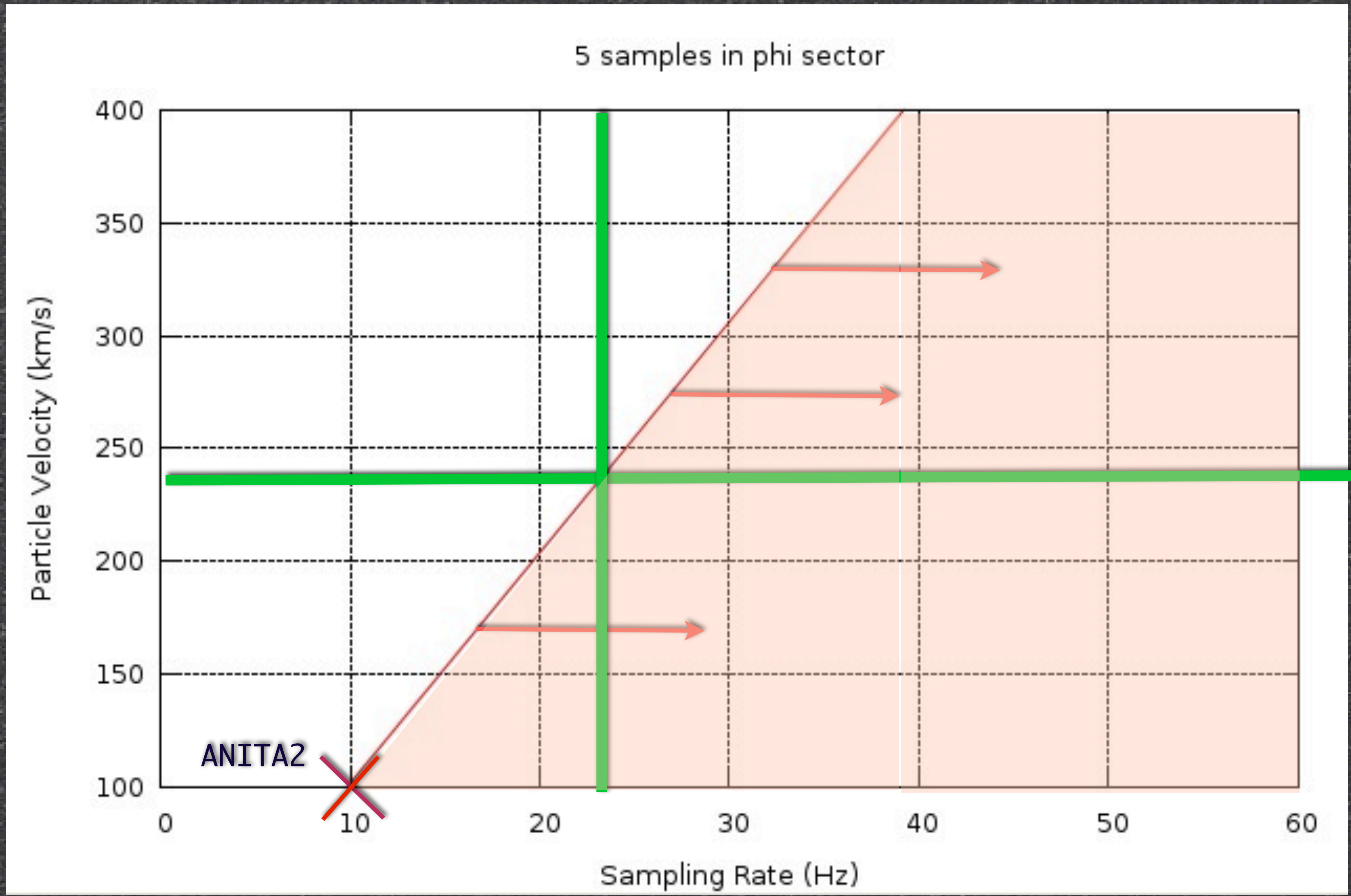

240km/s mean galactic velocity

Sensitivity Requirements

- Requires 0.2K sensitivity over 300K nominal noise environment
- 0.0029dB variation

from Gorham arxiv paper

RF Signal Path

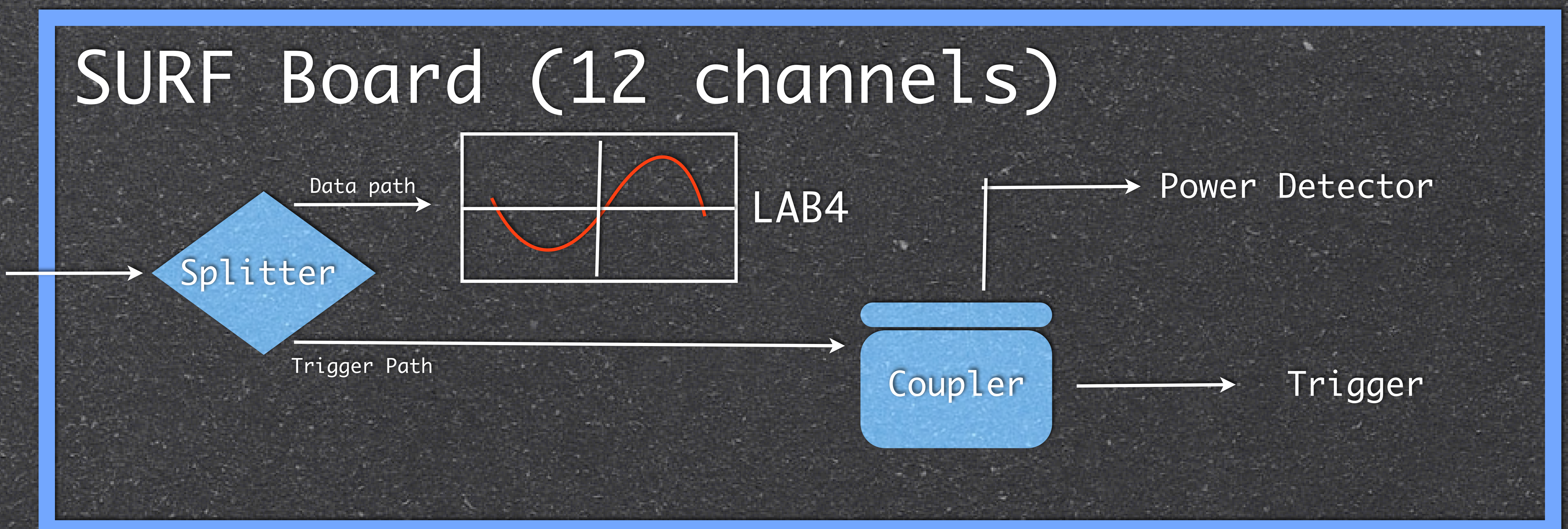

Expected Power

KTB=(1.38e-23[J/K])(300[K])(1e9[Hz])

=4.14nW   -83.8dBm

net gain {
+76dB of front end gain
-3dB splitter
-3dB/-10dB coupler

+63dB to Power Monitor → -20.8dBm

+73dB to Digitizer → -10.8dBm

+70dB to Digitizer → -13.8dBm

LTC5582 Power Detector

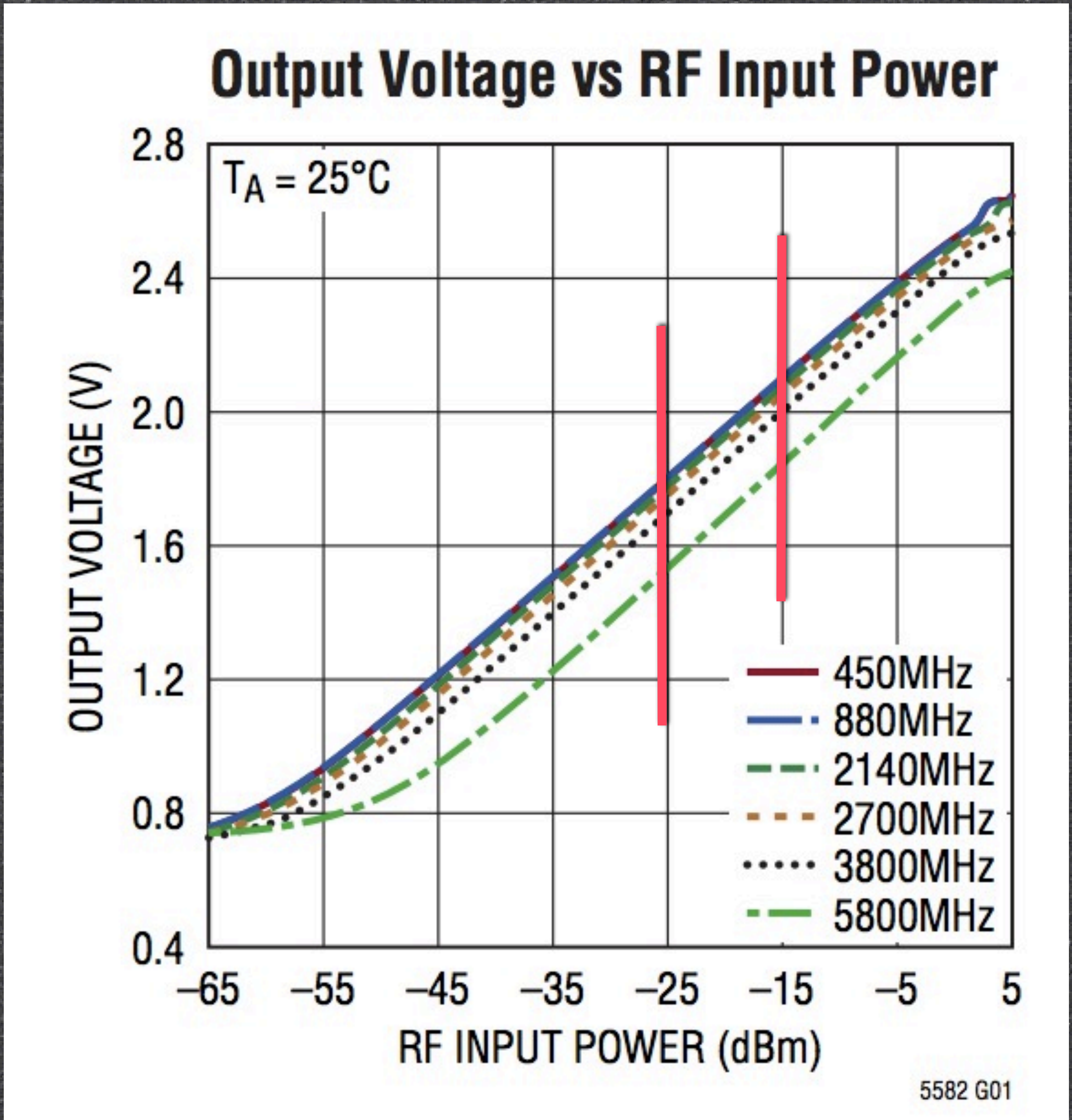

Linearly converts broadband RF power to digitizable voltage output

Resolution obtainable from OTS ADC

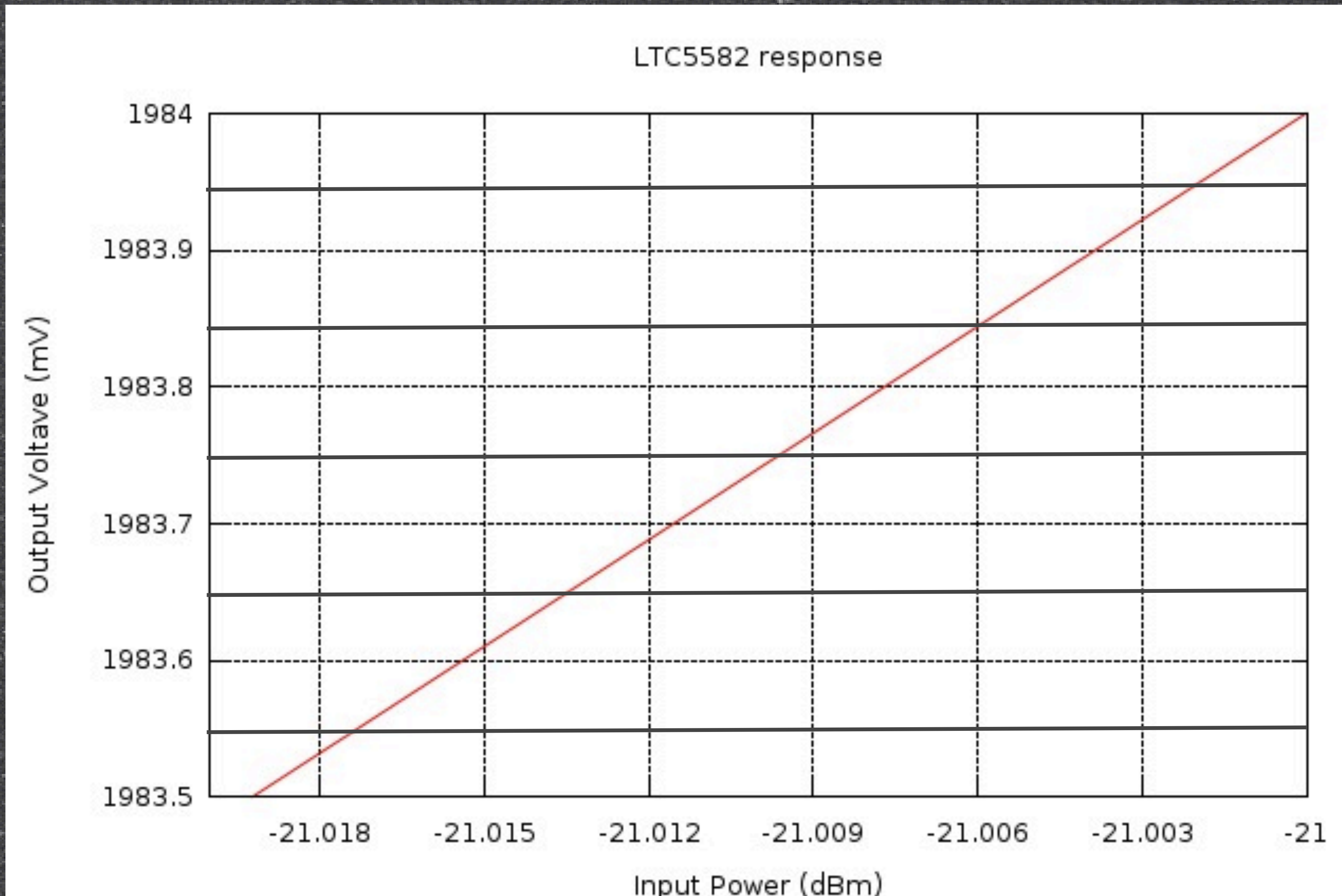

16bit digitizer (ADS1113)

2.5V/(2**16)=0.04mV

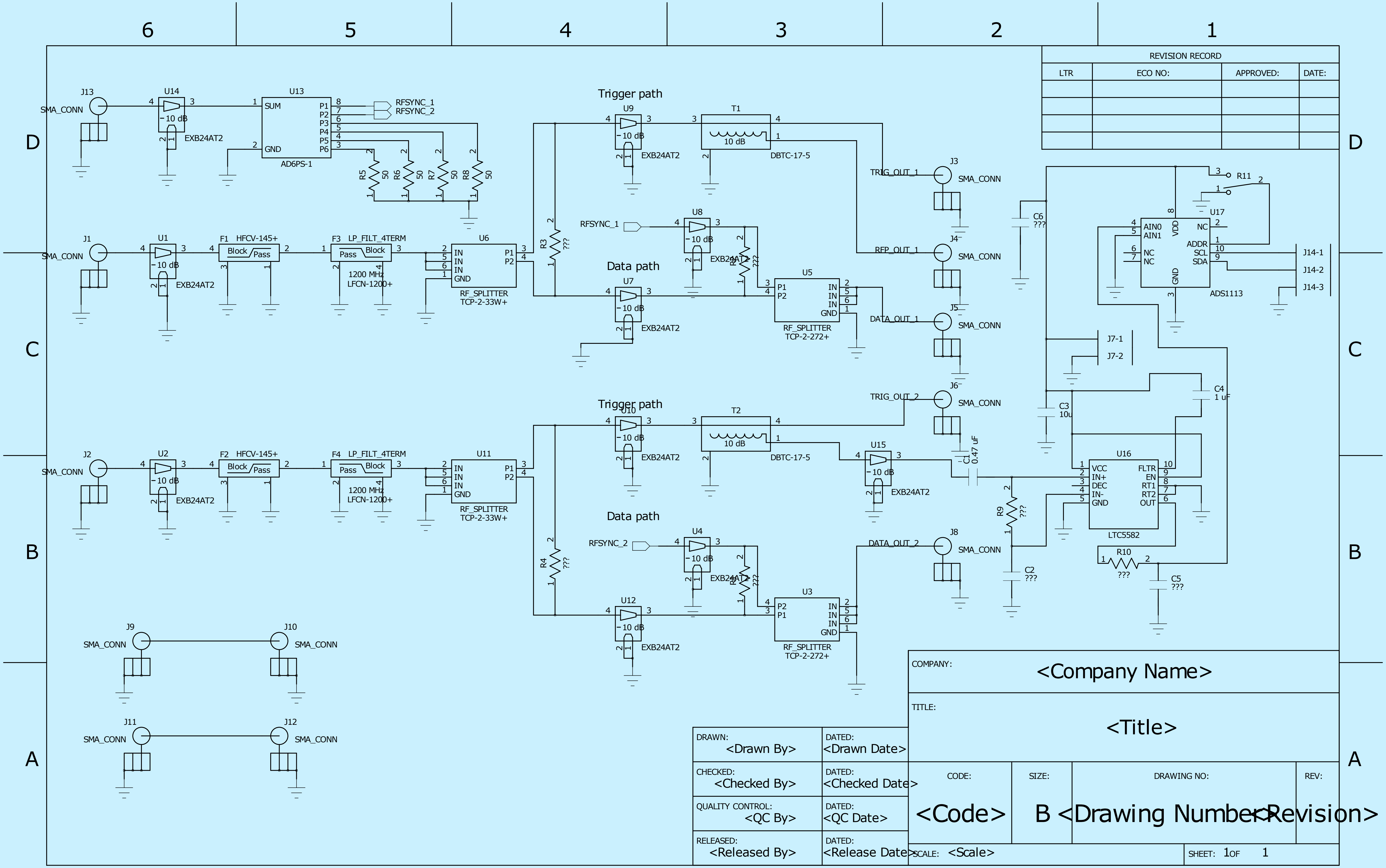
6
5
4
3
2
1
D
C
B
A
REVISION RECORD
LTR
ECO NO:
APPROVED:
DATE:
J13
SMA_CONN
U14
10 dB
EXB24AT2
U13
SUM
GND
P1
P2
P3
P4
P5
P6
AD6PS-1
RFSYNC_1
RFSYNC_2
R5
R6
R7
R8
50
Trigger path
U9
T1
DBTC-17-5
TRIG_OUT_1
J3
RFP_OUT_1
J4
Data path
U7
U8
RFSYNC_1
U5
RF_SPLITTER
TCP-2-272+
DATA_OUT_1
J5
J1
U1
F1
HFCV-145+
Block
Pass
F3
LP_FILT_4TERM
1200 MHz
LFCN-1200+
U6
IN
P1
P2
RF_SPLITTER
TCP-2-33W+
R3
???
C6
J7-1
J7-2
U17
AIN0
AIN1
NC
VDD
ADDR
SCL
SDA
ADS1113
R11
J14-1
J14-2
J14-3
C3
10u
C4
1 uF
Trigger path
U10
T2
TRIG_OUT_2
J6
C1
0.47 uF
U15
U16
VCC
IN+
DEC
IN-
FLTR
EN
RT1
RT2
OUT
LTC5582
R9
R10
C2
C5
Data path
U4
RFSYNC_2
U12
U3
DATA_OUT_2
J8
R4
J2
U2
F2
F4
U11
J9
J10
J11
J12
COMPANY:
<Company Name>
TITLE:
<Title>
DRAWN:
<Drawn By>
DATED:
<Drawn Date>
CHECKED:
<Checked By>
<Checked Date>
QUALITY CONTROL:
<QC By>
<QC Date>
RELEASED:
<Released By>
<Release Date>
CODE:
<Code>
SIZE:
B
DRAWING NO:
<Drawing Number>
REV:
<Revision>
SCALE:
<Scale>
SHEET: 1 OF 1

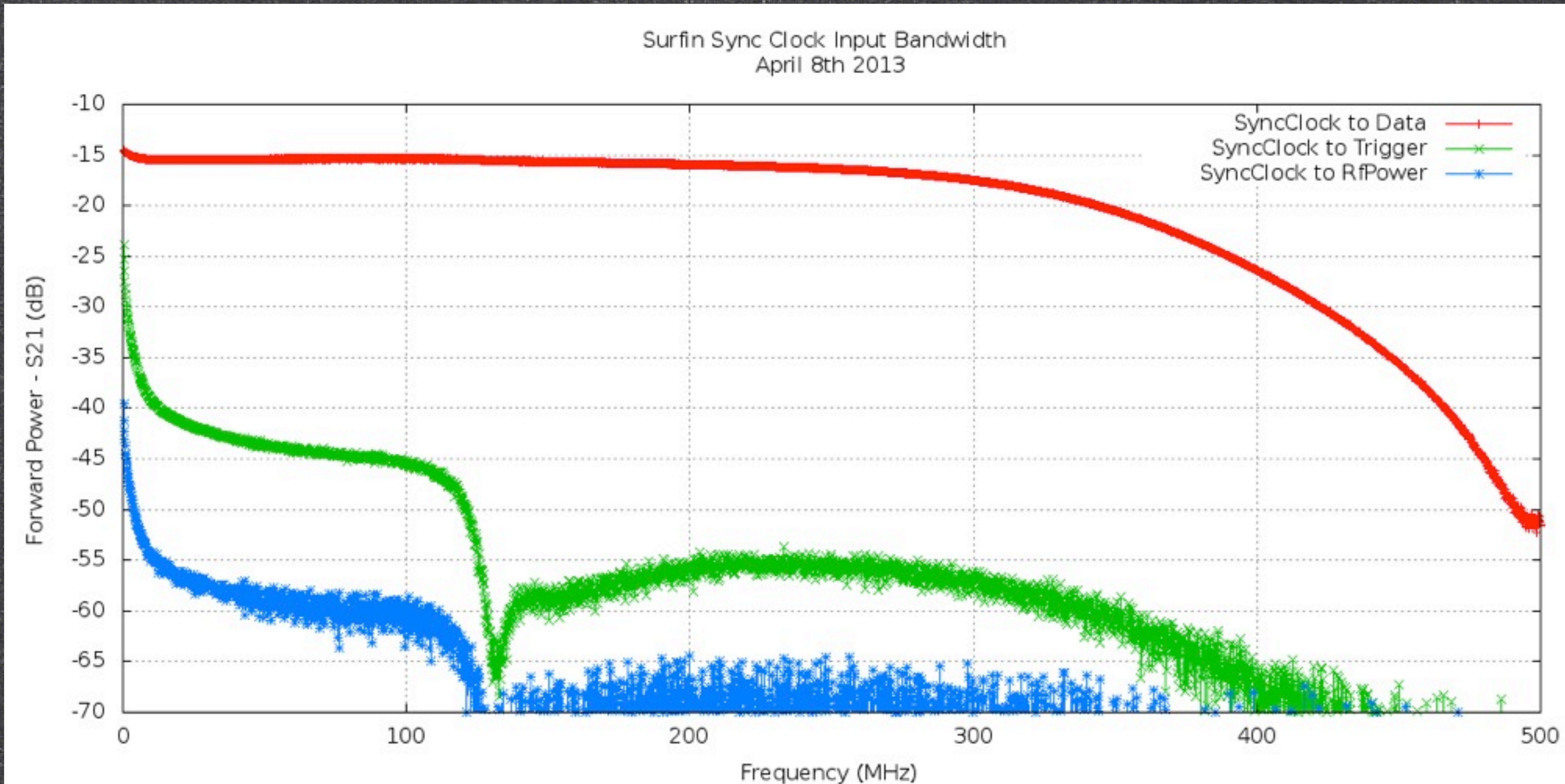
Surfin Sync Clock Input Bandwidth
April 8th 2013
SyncClock to Data
SyncClock to Trigger
SyncClock to RfPower
Forward Power - S21 (dB)
Frequency (MHz)
-10
-15
-20
-25
-30
-35
-40
-45
-50
-55
-60
-65
-70
0
100
200
300
400
500

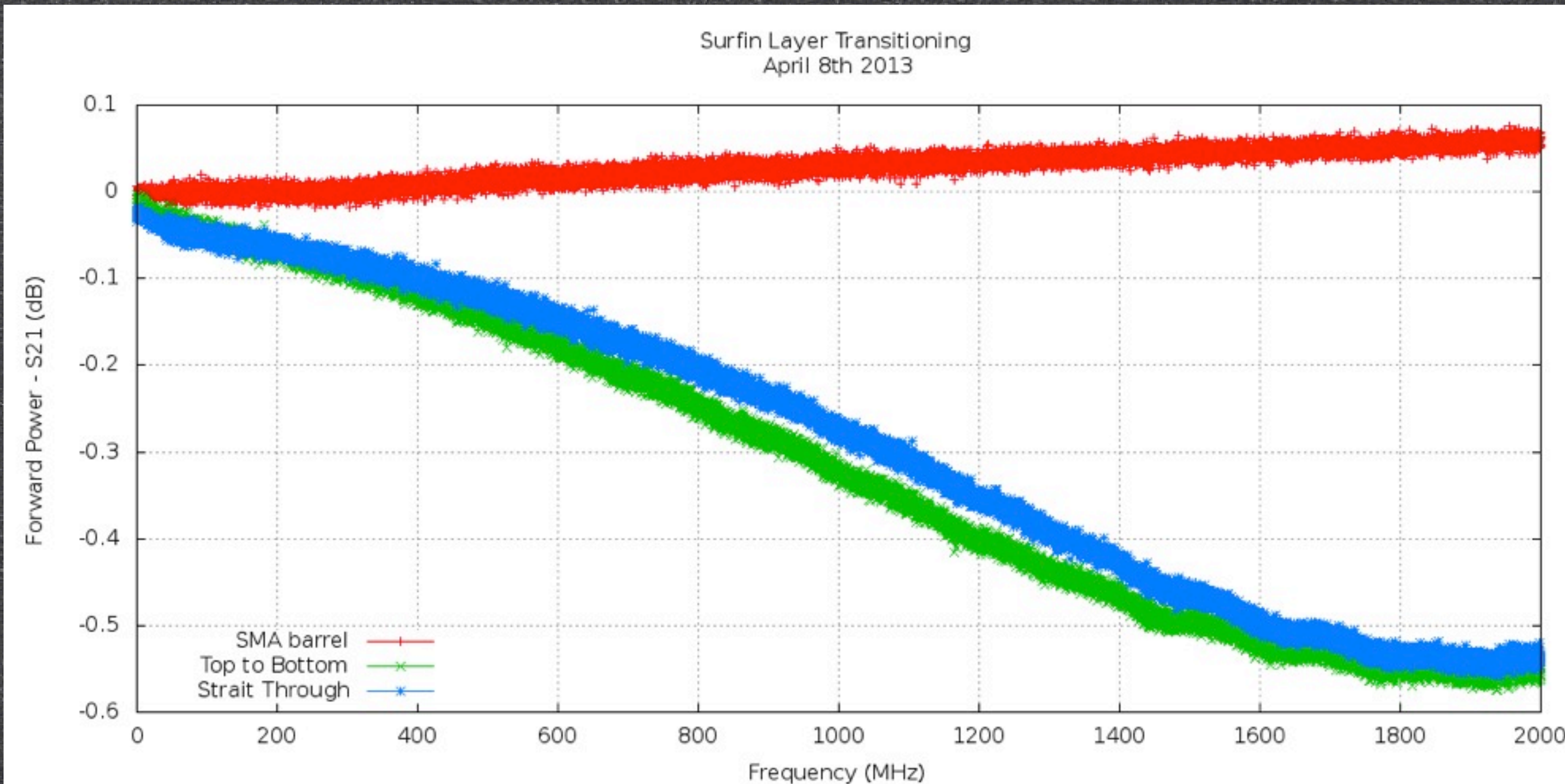
Surfin Layer Transitioning
April 8th 2013
Forward Power - S21 (dB)
Frequency (MHz)
SMA barrel
Top to Bottom
Strait Through
0.1
0
-0.1
-0.2
-0.3
-0.4
-0.5
-0.6
0
200
400
600
800
1000
1200
1400
1600
1800
2000

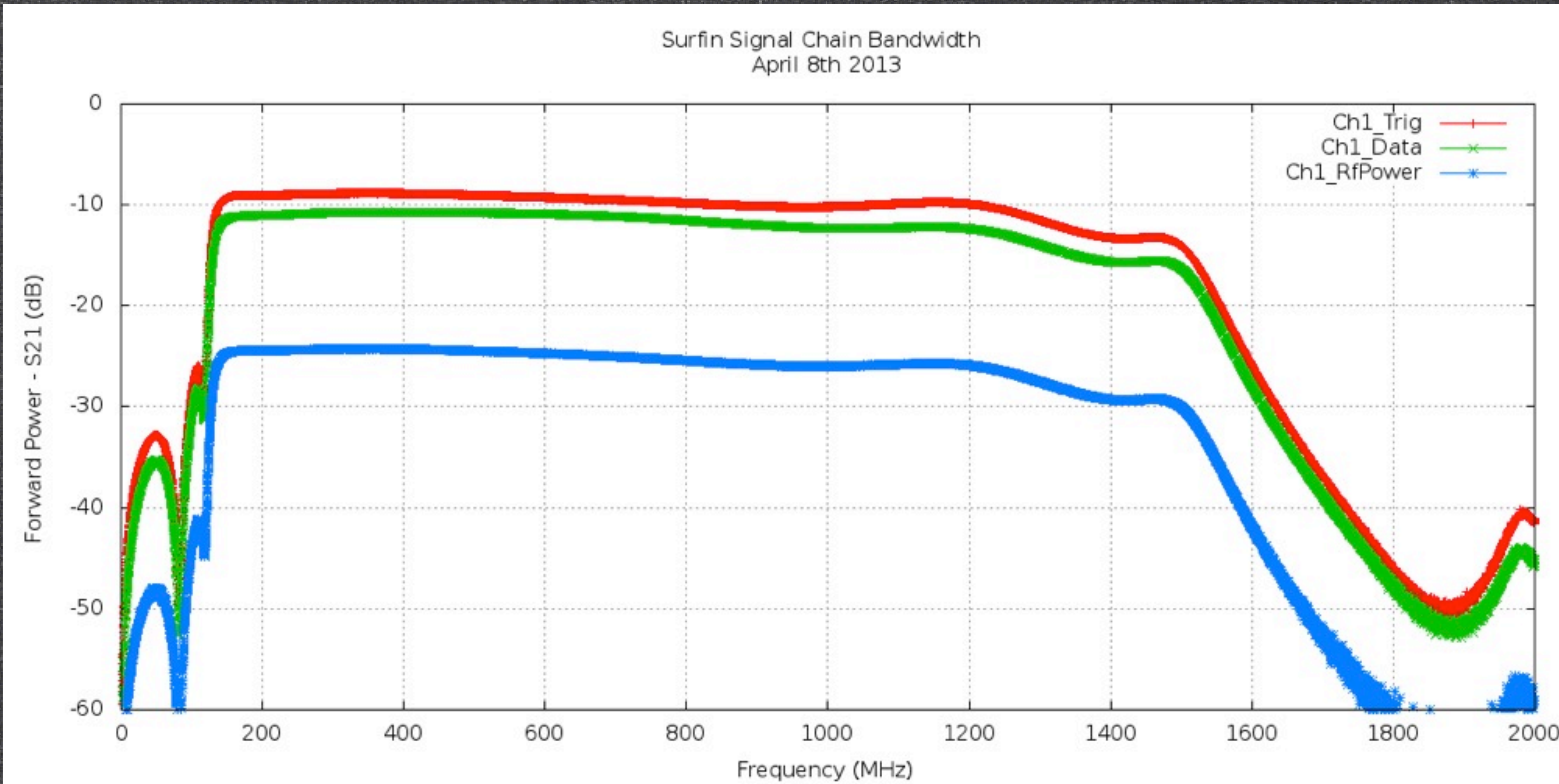
Surfin Signal Chain Bandwidth
April 8th 2013
Ch1_Trig
Ch1_Data
Ch1_RfPower
Forward Power - S21 (dB)
Frequency (MHz)
0
-10
-20
-30
-40
-50
-60
0
200
400
600
800
1000
1200
1400
1600
1800
2000

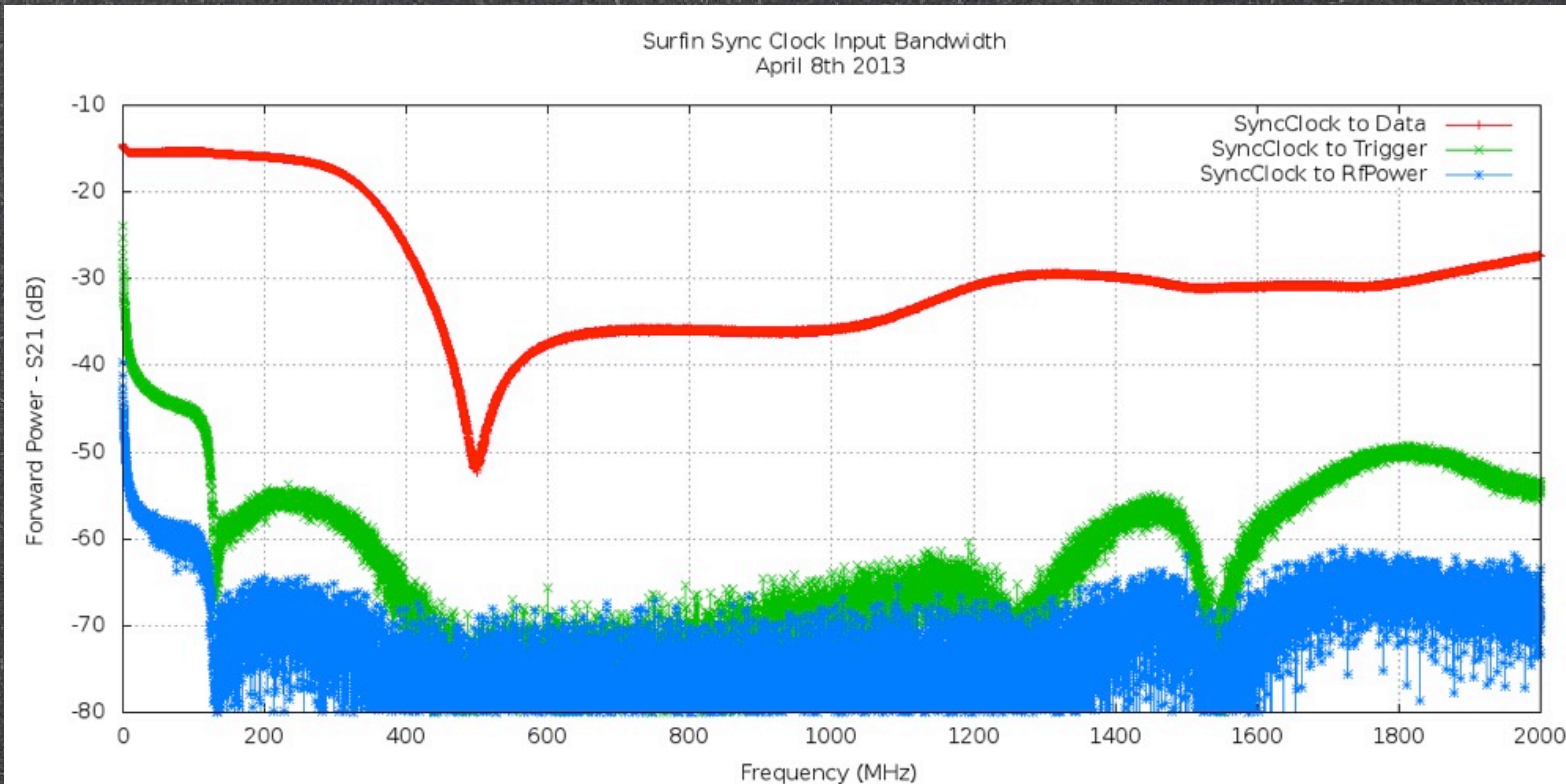
Surfin Sync Clock Input Bandwidth
April 8th 2013
SyncClock to Data
SyncClock to Trigger
SyncClock to RfPower
Forward Power - S21 (dB)
Frequency (MHz)
-10
-20
-30
-40
-50
-60
-70
-80
0
200
400
600
800
1000
1200
1400
1600
1800
2000

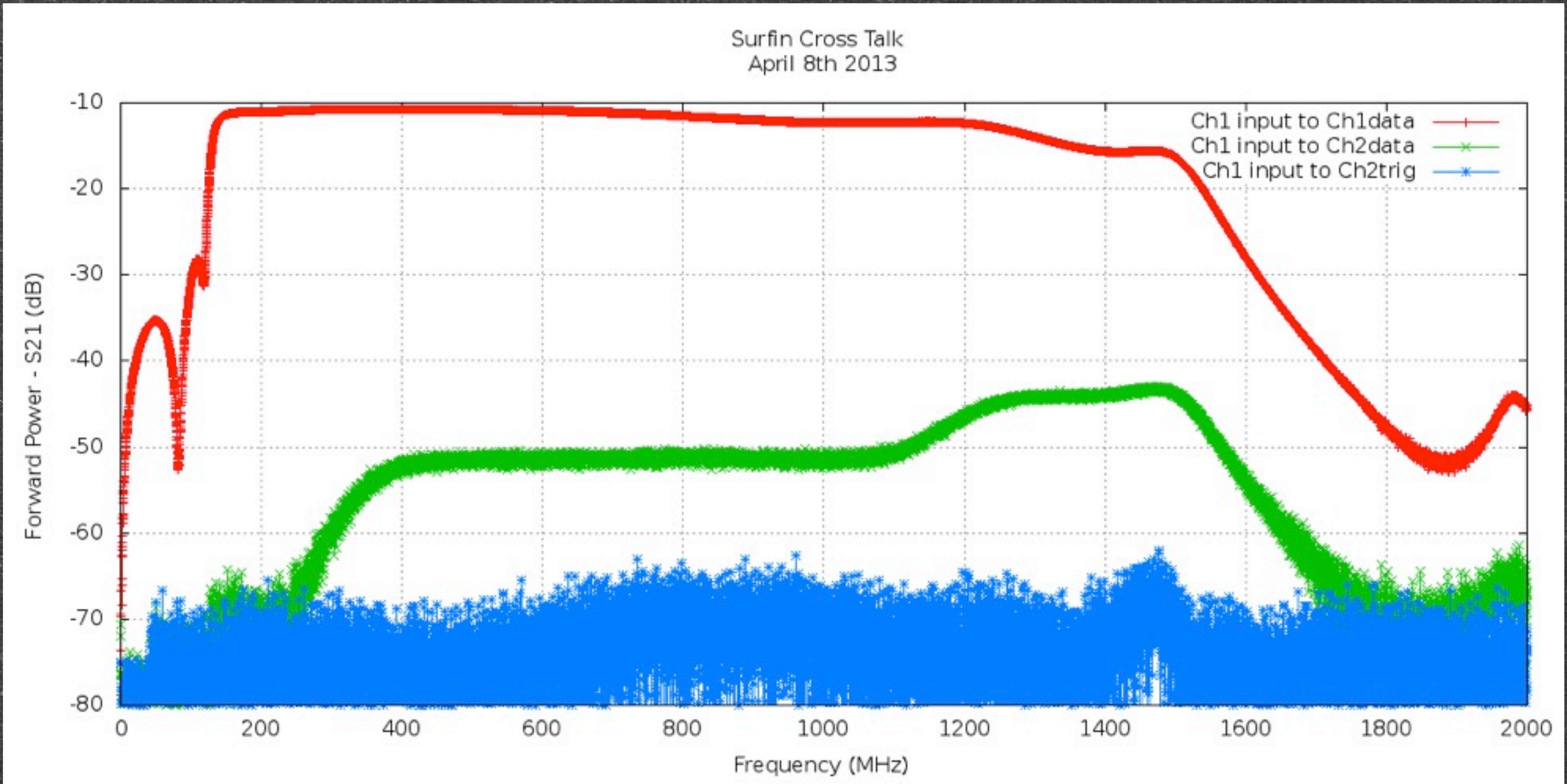
Surfin Cross Talk
April 8th 2013
Forward Power - S21 (dB)
Frequency (MHz)
Ch1 input to Ch1data
Ch1 input to Ch2data
Ch1 input to Ch2trig
-10
-20
-30
-40
-50
-60
-70
-80
0
200
400
600
800
1000
1200
1400
1600
1800
2000

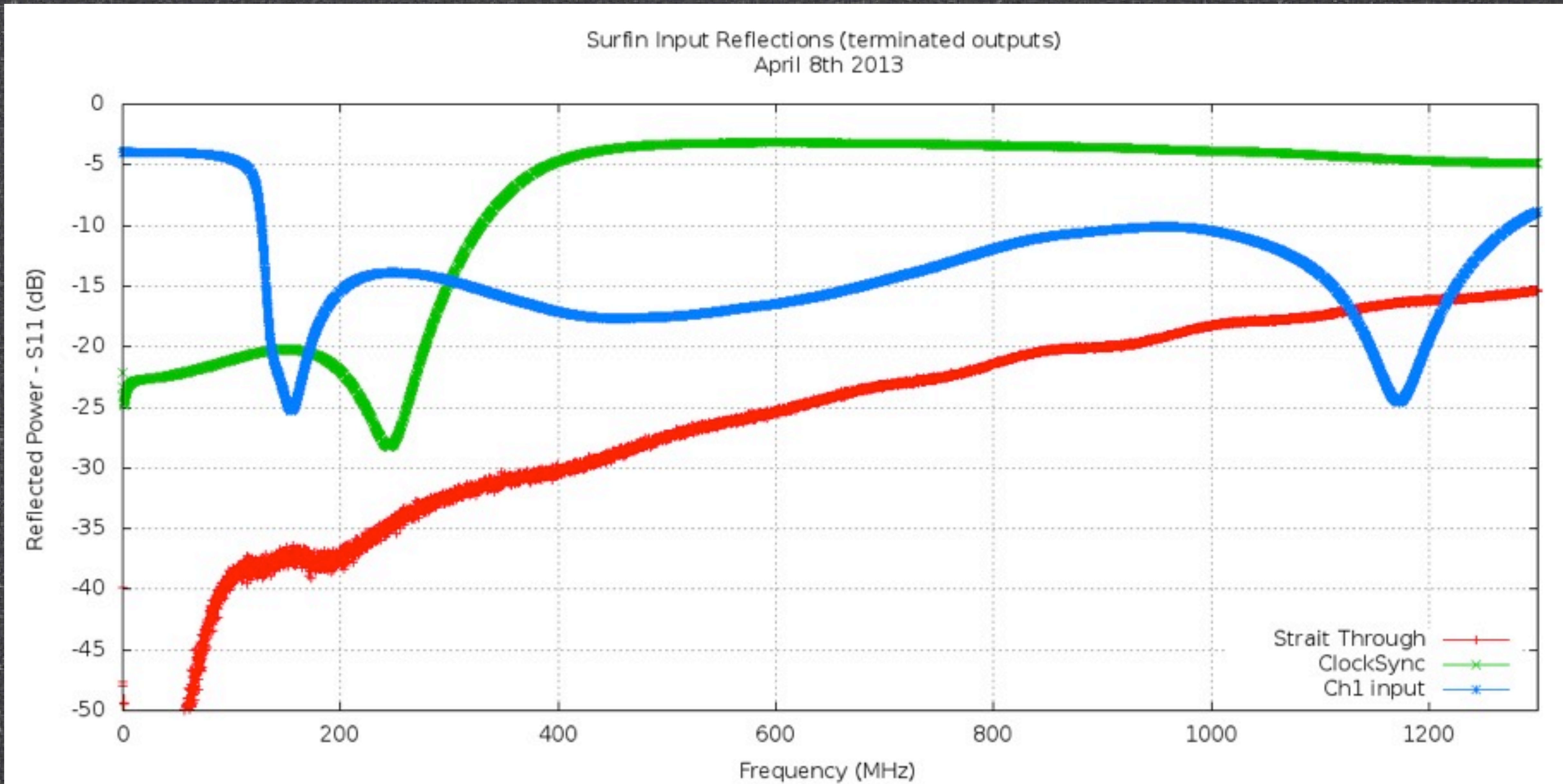

Surfin Input Reflections (terminated outputs)
April 8th 2013
Reflected Power - S11 (dB)
0
-5
-10
-15
-20
-25
-30
-35
-40
-45
-50
0
200
400
600
800
1000
1200
Frequency (MHz)
Strait Through
ClockSync
Ch1 input

Surfin Power Detector Circuit

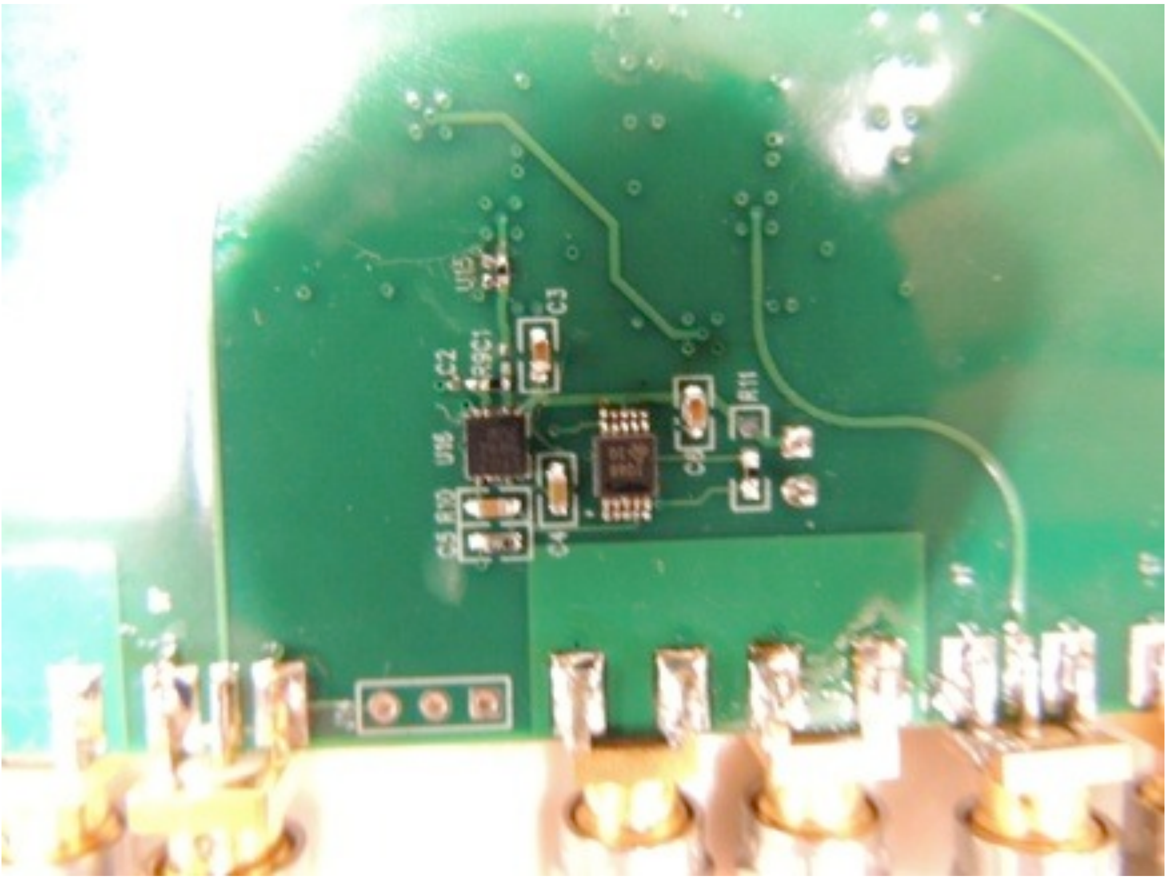

From Trigger Path

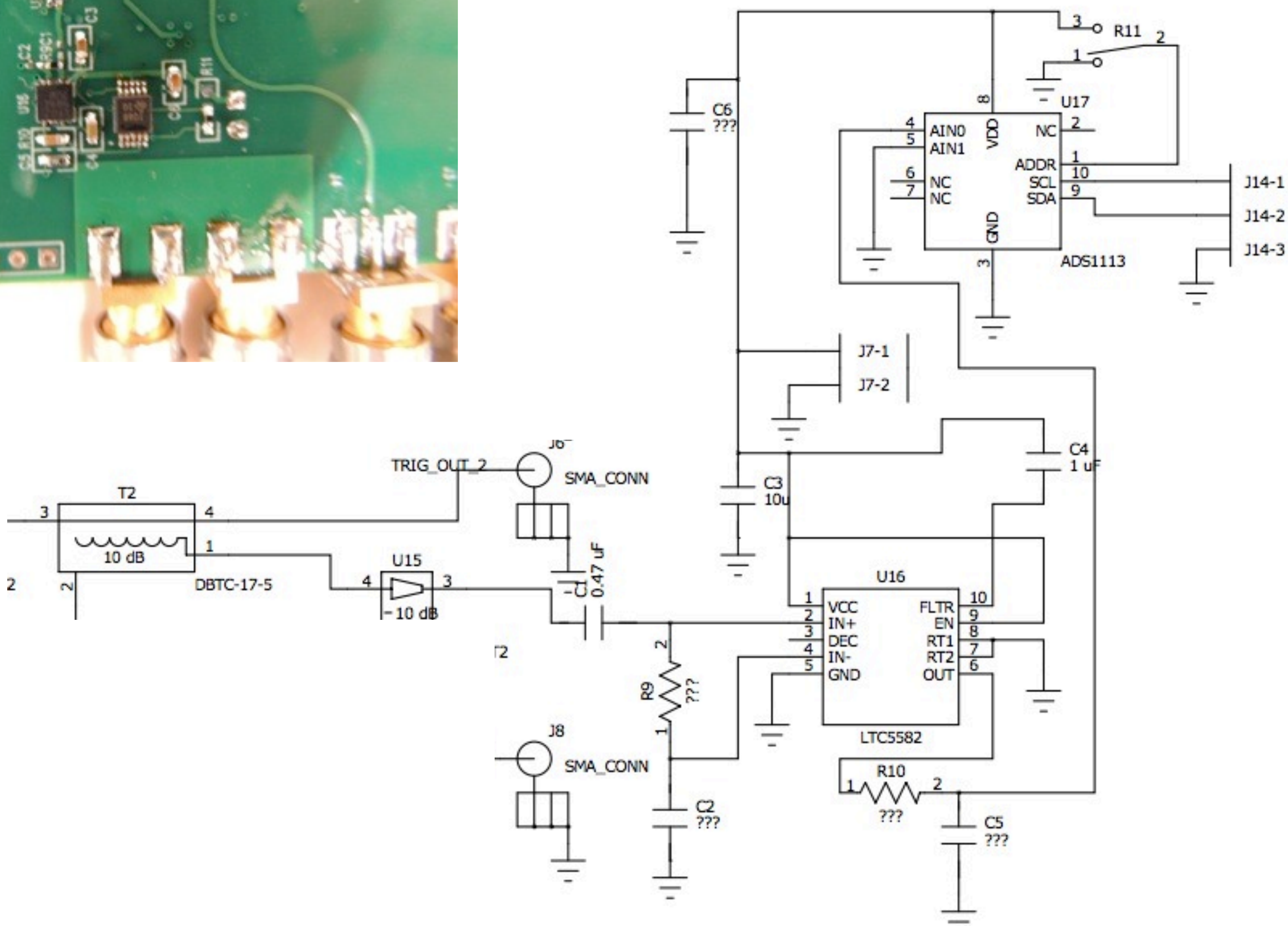

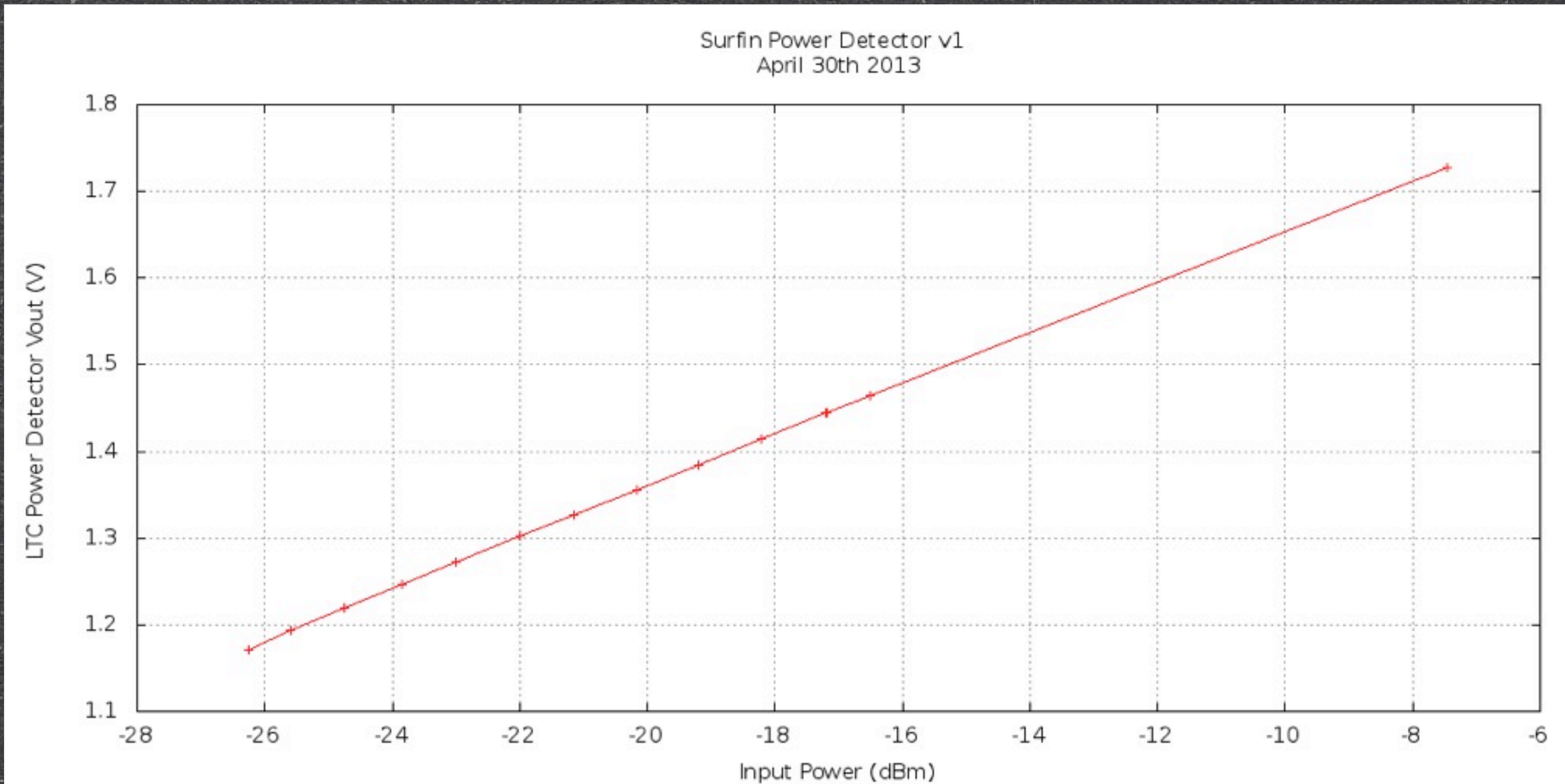
Surfin Power Detector v1
April 30th 2013
LTC Power Detector Vout (V)
1.8
1.7
1.6
1.5
1.4
1.3
1.2
1.1
-28
-26
-24
-22
-20
-18
-16
-14
-12
-10
-8
-6
Input Power (dBm)

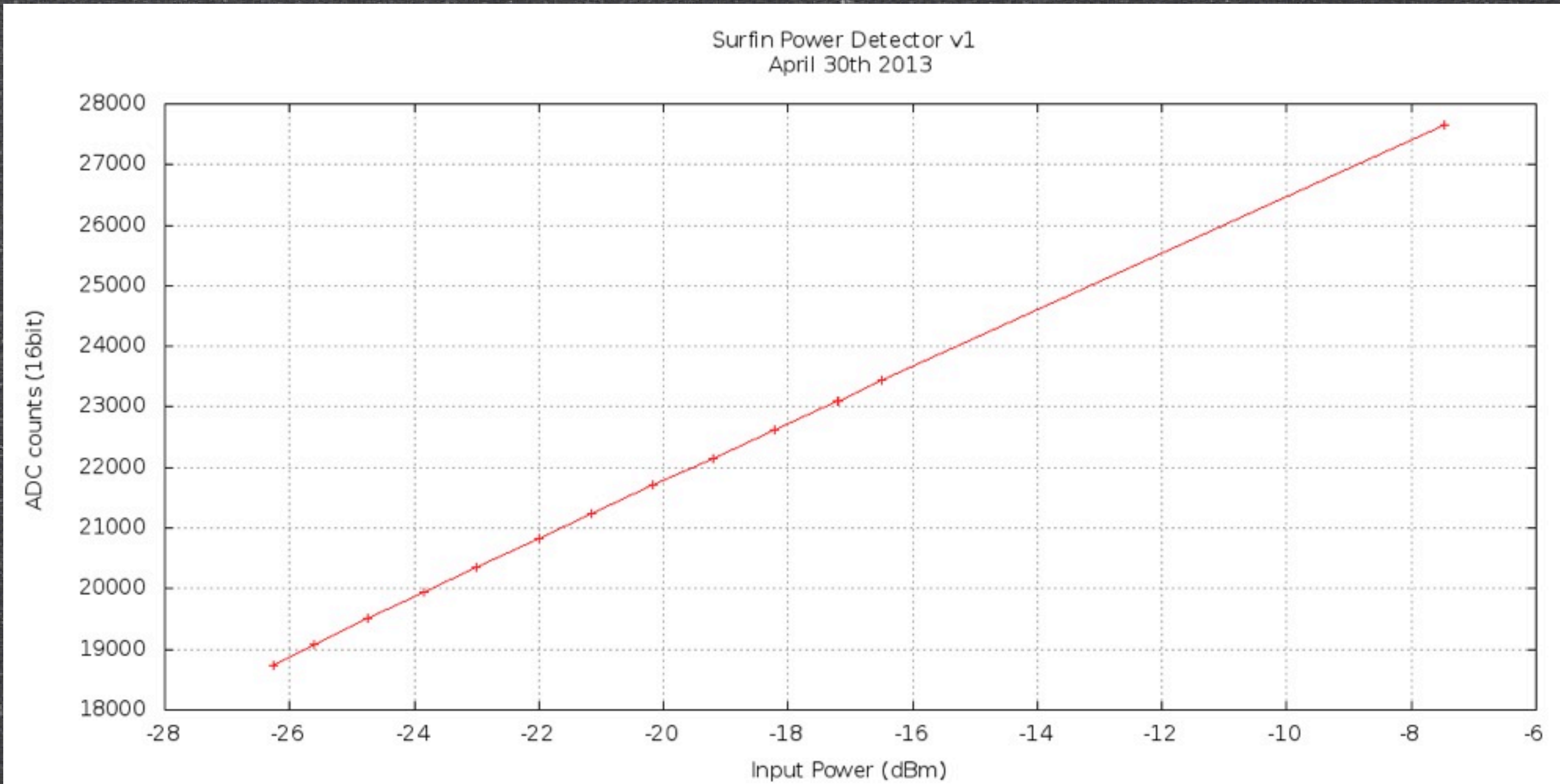
Surfin Power Detector v1
April 30th 2013
ADC counts (16bit)
28000
27000
26000
25000
24000
23000
22000
21000
20000
19000
18000
-28
-26
-24
-22
-20
-18
-16
-14
-12
-10
-8
-6
Input Power (dBm)

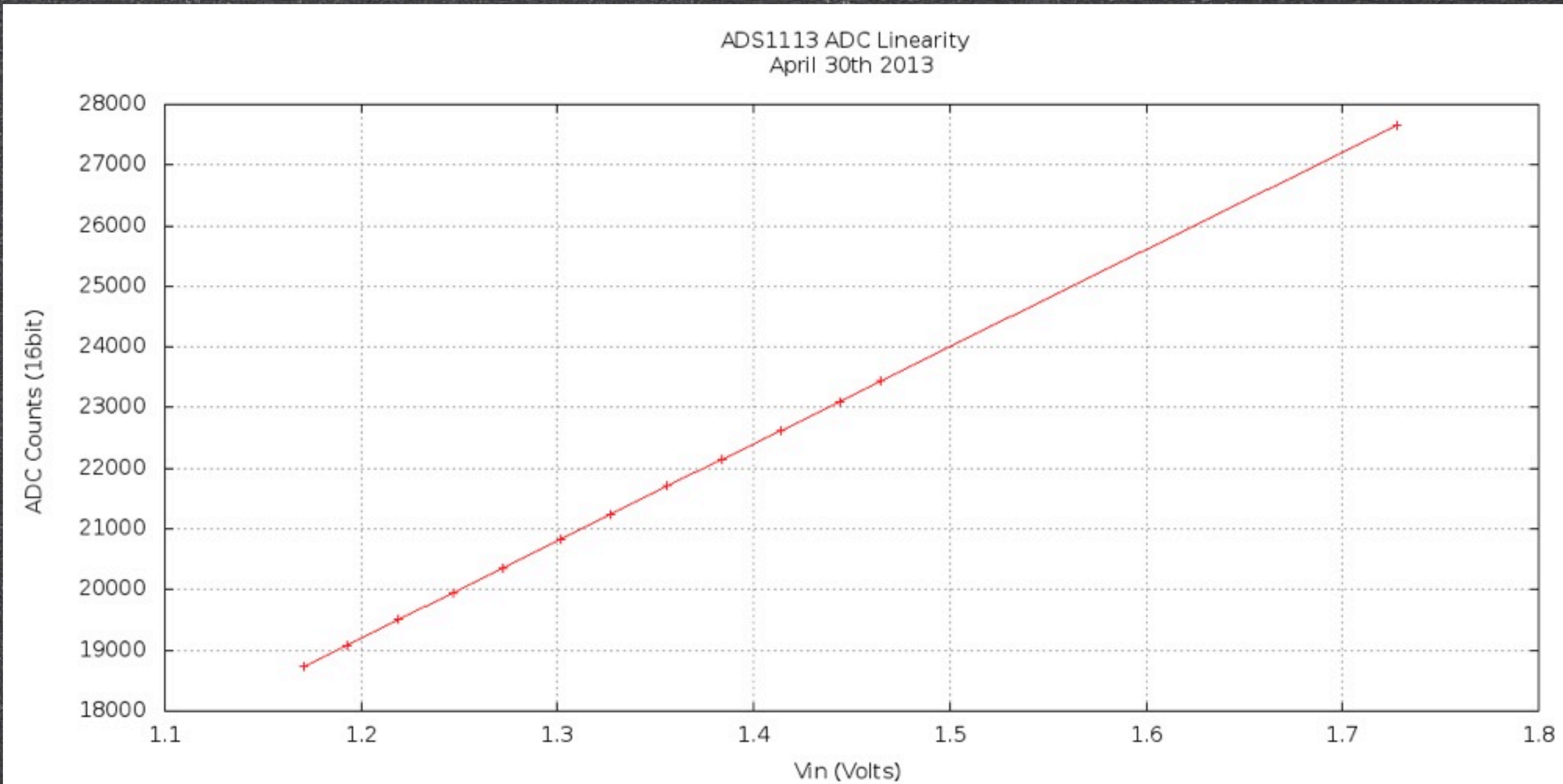
ADS1113 ADC Linearity
April 30th 2013
28000
27000
26000
25000
24000
23000
22000
21000
20000
19000
18000
ADC Counts (16bit)
1.1
1.2
1.3
1.4
1.5
1.6
1.7
1.8
Vin (Volts)

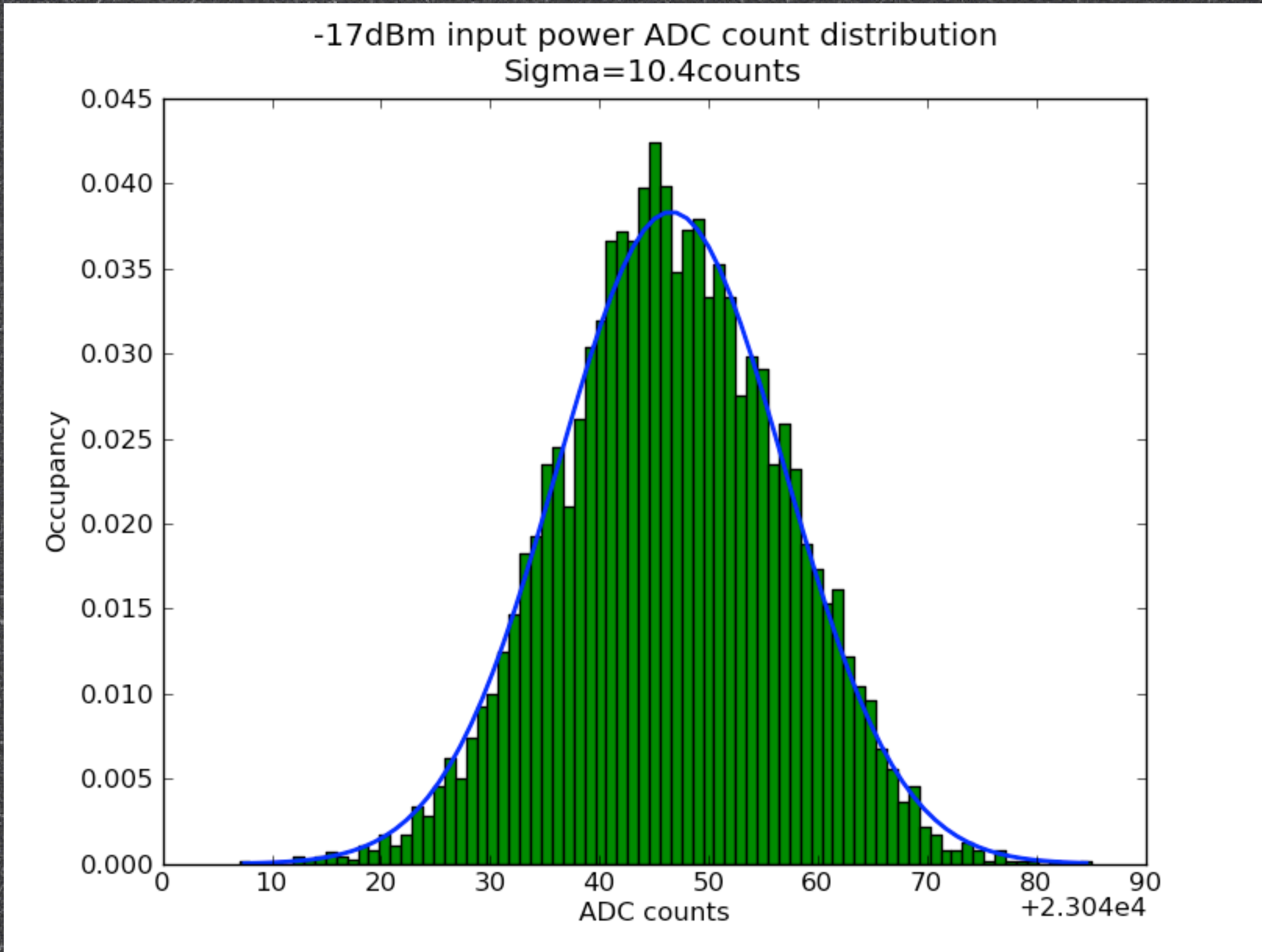
-17dBm input power ADC count distribution
Sigma=10.4counts
0.045
0.040
0.035
0.030
0.025
0.020
0.015
0.010
0.005
0.000
Occupancy
0
10
20
30
40
50
60
70
80
90
ADC counts
+2.304e4

Conclusion

- ANITA-3 mission already a go, additional science for minimal resource and time investment
- Further constrains possible dark matter candidates
- Directional and energy measurements possible.

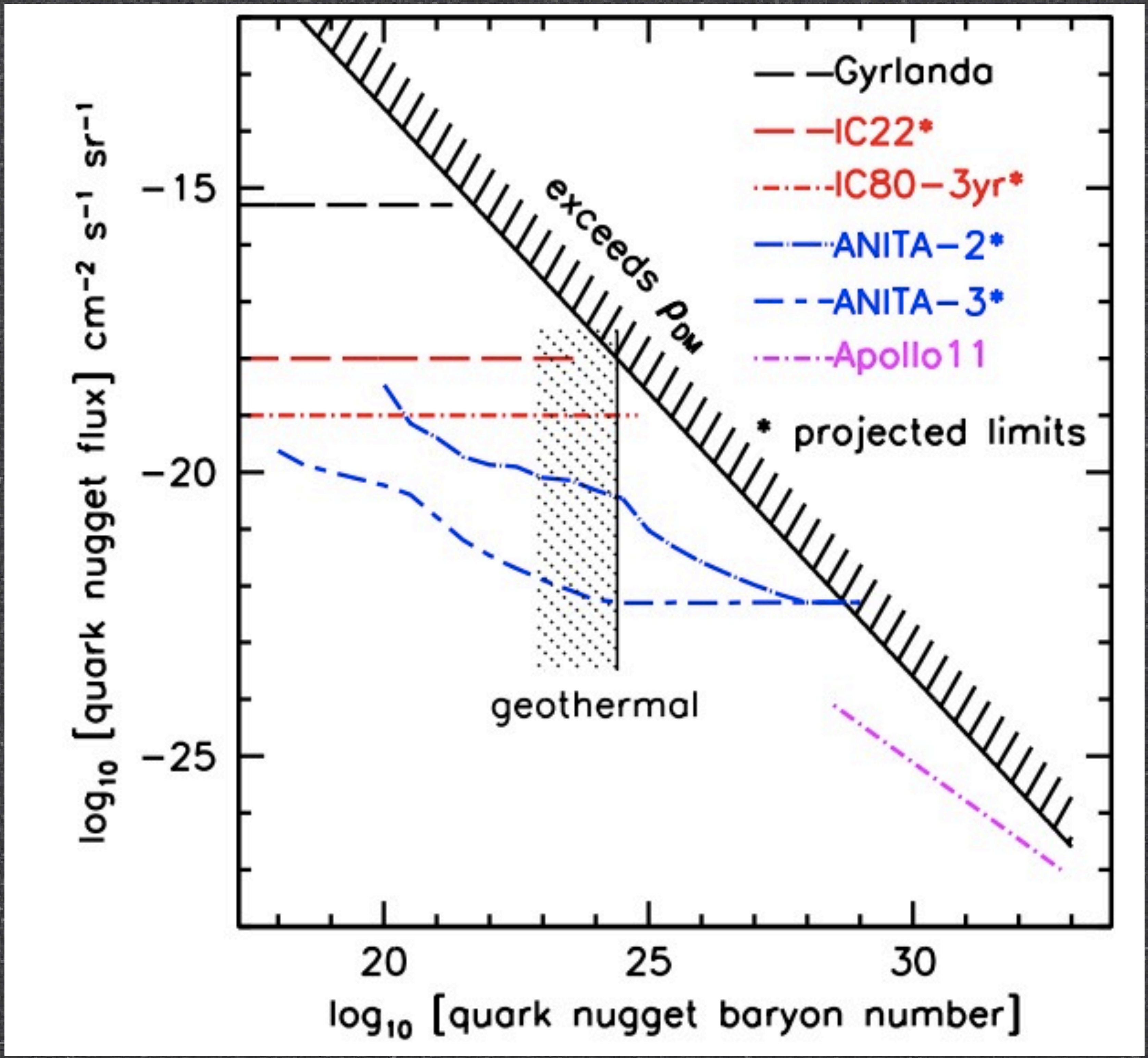

Extra slides

Useful purposes for RF power monitor circuit

- Slow RF data monitor
  - Can be used to determine channel by channel operational status without relying on LAB4 or RITC
- Rough orientation sensor
  - Can use absolute power measurement to determine sun position

Production Mechanism

- Remanent of quantum chromodynamic phase transition in early universe evolution
- Neutral and metastable during formation
- Avoid nucleosynthesis interactions (baryonic content constraint avoided)
- Possible stability provided by “color superconductivity” at Fermi surface of nugget

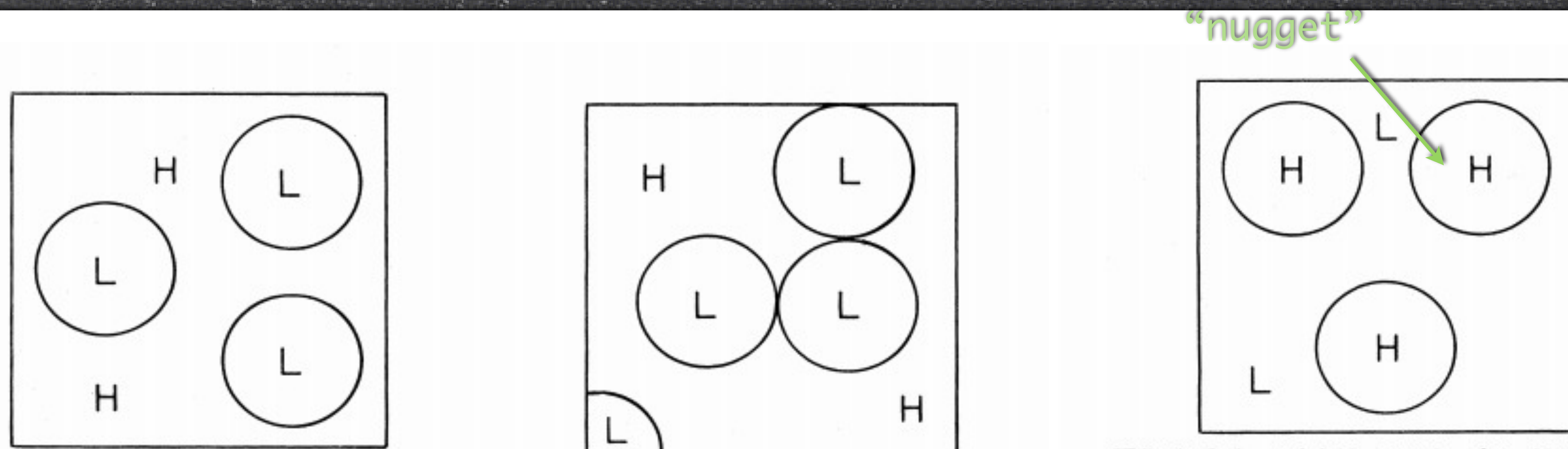

FIG. 1. Isolated expanding bubbles of low-temperature phase in the high-temperature phase.

FIG. 2. The expanding bubbles meet.

FIG. 3. Isolated shrinking bubbles of the high-temperature phase.

E. Witten, Phys. Rev. D 30, 272 (1984)

Storage requirements

2 bytes per event

x100 channels

-> 200 (bytes/second)/Hz

400Hz will yield 800kB/sec

(waveform readout 10x greater)

~400GB for 60 day flight

Azimuth response

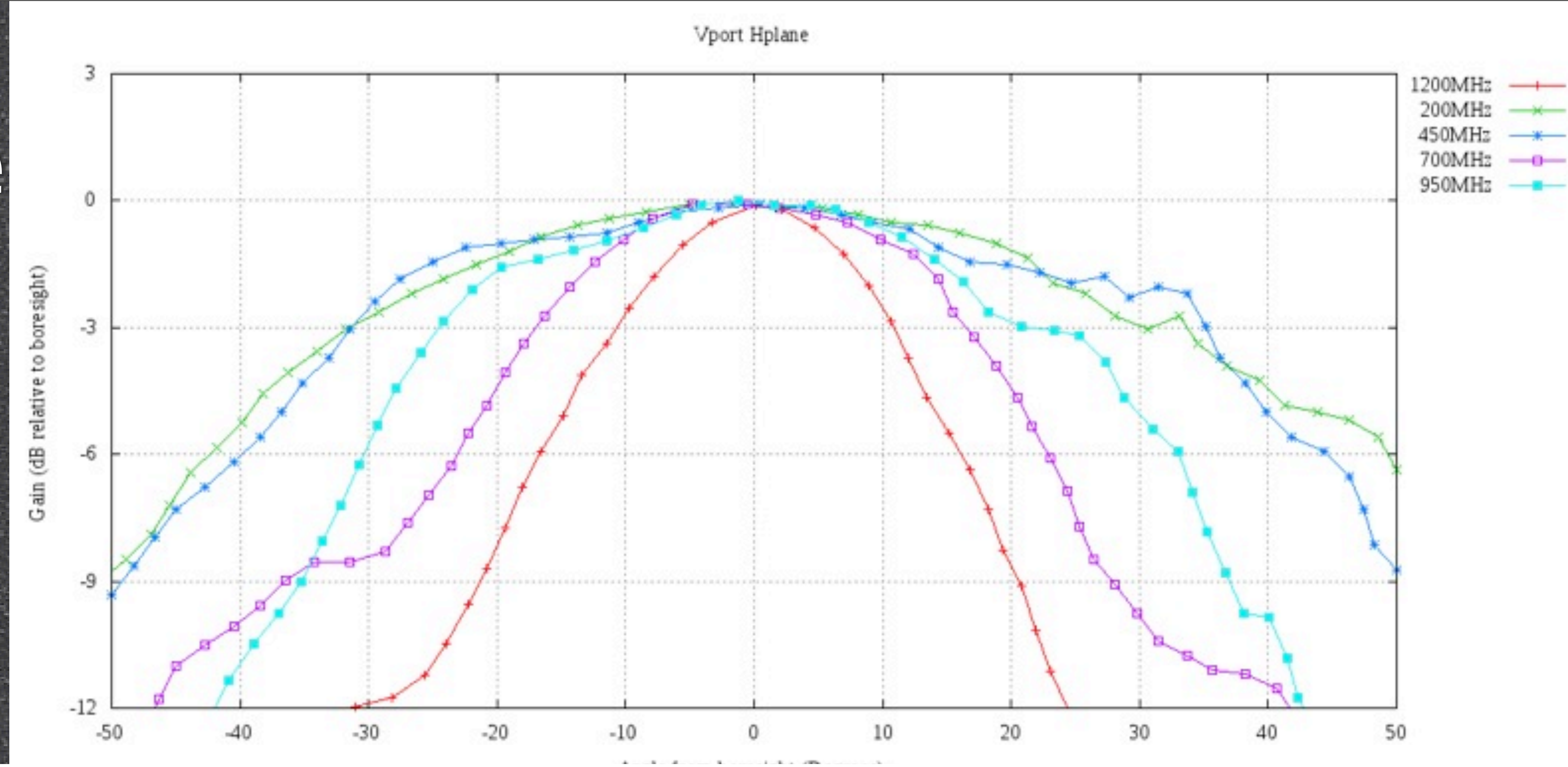

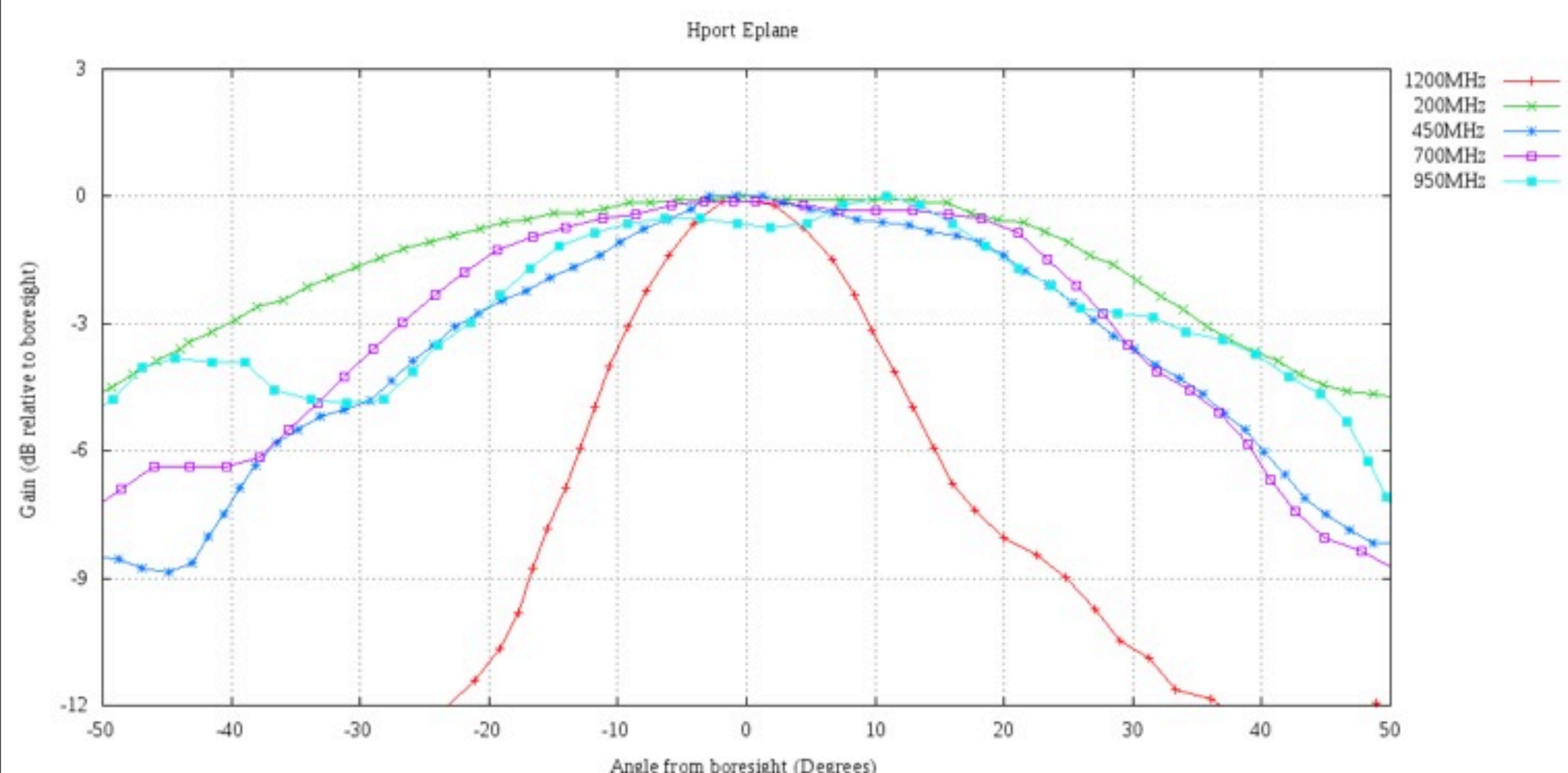

Elevation response

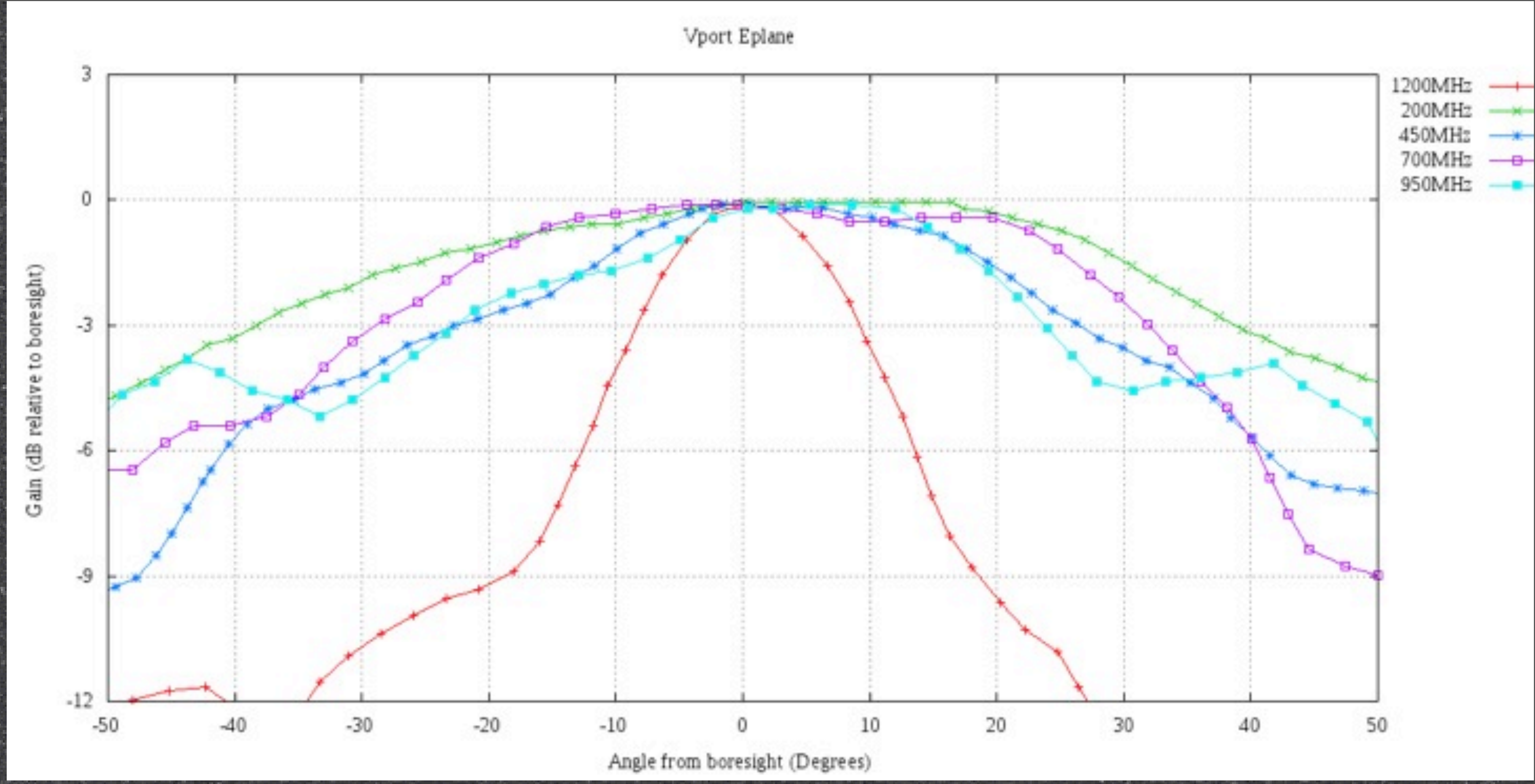

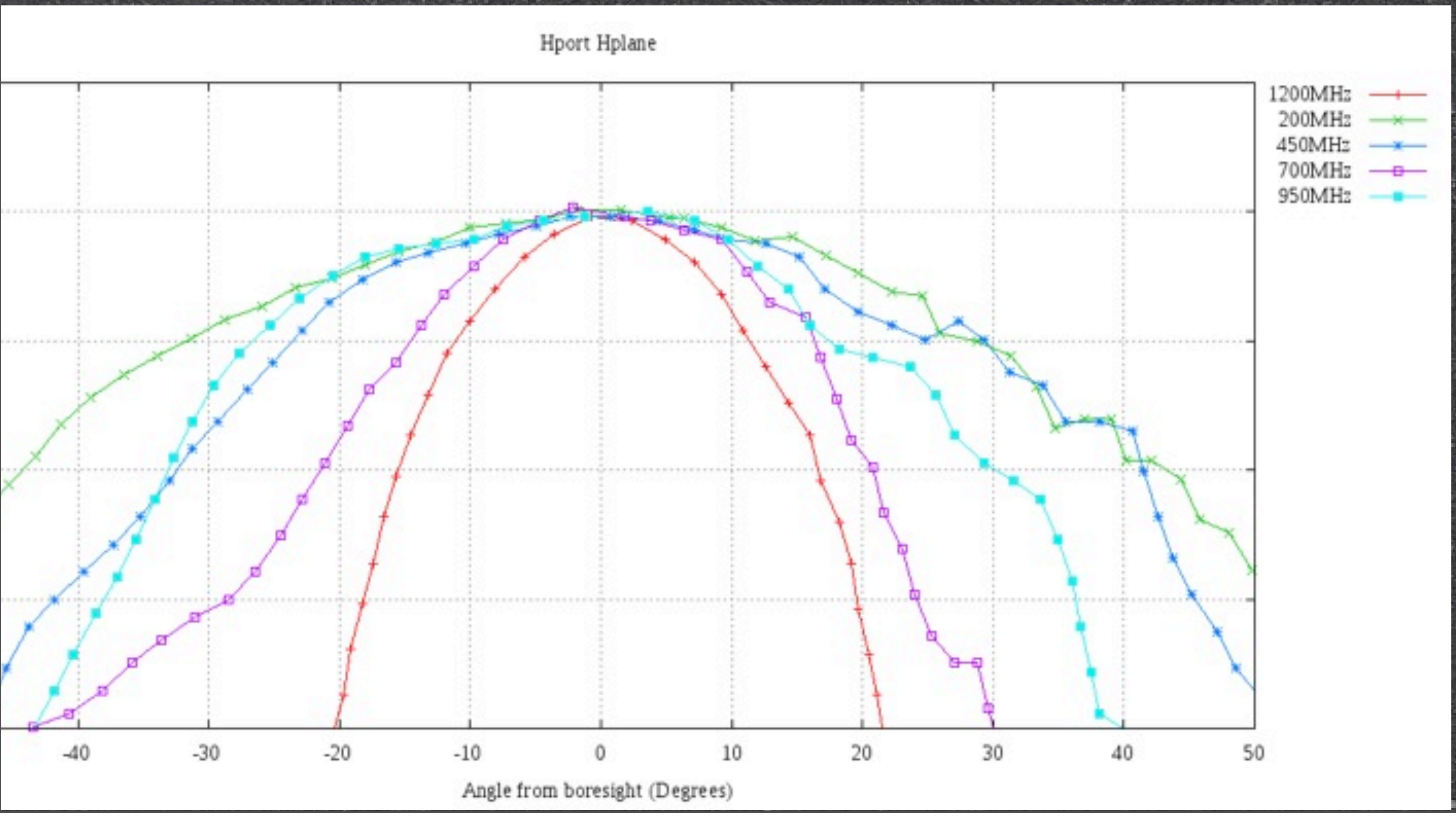

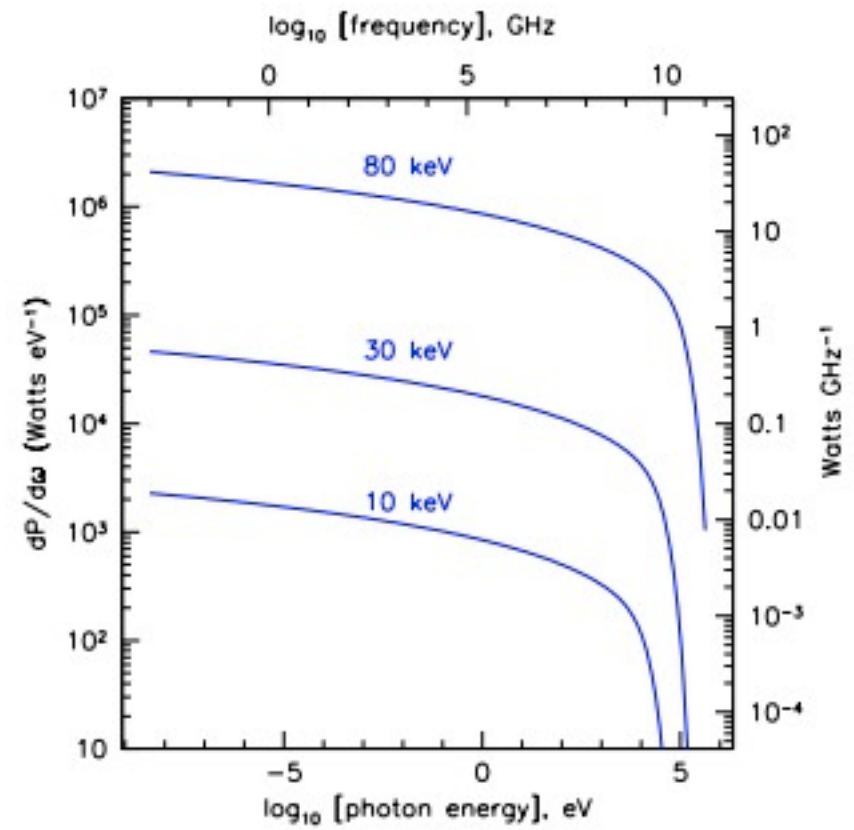

FIG. 1: *Spectral density of emission from a* $B \sim 10^{24}$ *antiquark nugget for three values of the effective surface temperature.*

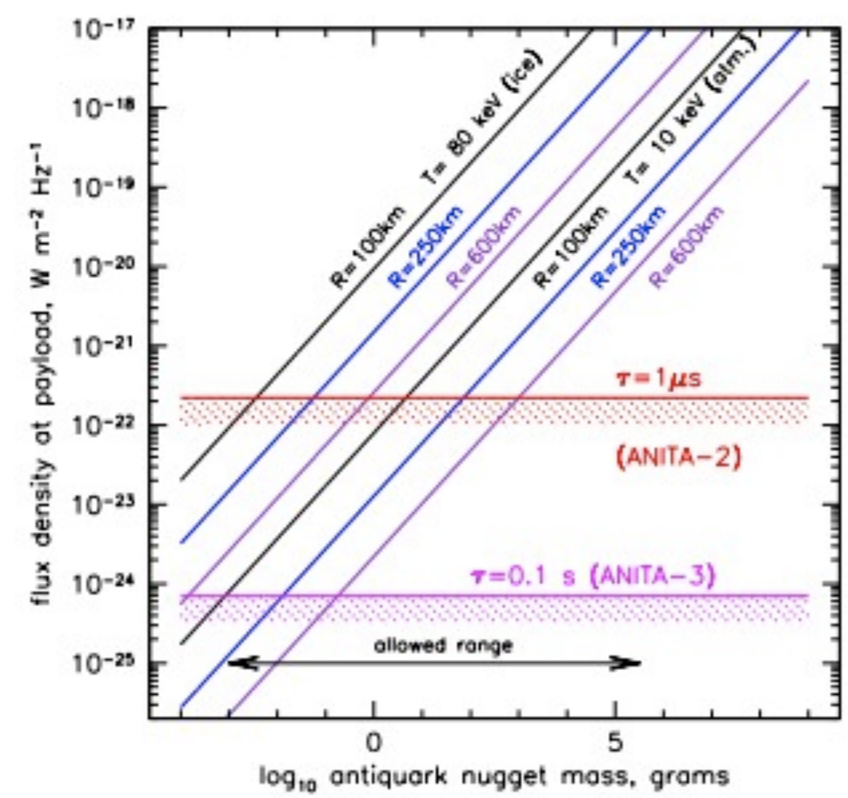

FIG. 2: *Estimated flux density and sensitivity for ANITA for two different AQN temperatures and three different distances, for AQN transiting in atmosphere (*$T = 10$ *keV), or Antarctic ice (*$T = 80$ *keV), with typical estimated attenuation losses and Fresnel coefficient. The thermal noise levels for two different integration times are shown.*